NANO · MICRO small
www.small-journal.com

Plant-Actuated Micro–Nanorobotics Platforms: Structural Designs, Functional Prospects, and Biomedical Applications

*Rachmi Luthfikasari, Tejal V. Patil, Dinesh K. Patel, Sayan Deb Dutta, Keya Ganguly, Maria Mercedes Espinal, and Ki-Taek Lim**

Plants are anatomically and physiologically different from humans and animals; however, there are several possibilities to utilize the unique structures and physiological systems of plants and adapt them to new emerging technologies through a strategic biomimetic approach. Moreover, plants provide safe and sustainable results that can potentially solve the problem of mass-producing practical materials with hazardous and toxic side effects, particularly in the biomedical field, which requires high biocompatibility. In this review, it is investigated how micro–nanostructures available in plants (e.g., nanoparticles, nanofibers and their composites, nanoporous materials, and natural micromotors) are adapted and utilized in the design of suitable materials for a micro–nanorobot platform. How plants' work on micro- and nanoscale systems (e.g., surface roughness, osmotically induced movements such as nastic and tropic, and energy conversion and harvesting) that are unique to plants, can provide functionality on the platform and become further prospective resources are examined. Furthermore, implementation across organisms and fields, which is promising for future practical applications of the plant-actuated micro–nanorobot platform, especially on biomedical applications, is discussed. Finally, the challenges following its implementation in the micro–nanorobot platform are also presented to provide advanced adaptation in the future.

1. Introduction

Renewable resources continue to be the main focus of recent studies to provide eco-friendly, cost-effective alternative energy.[1,2] The demand for sustainable materials are high because they reduce the amount of materials required to develop systems with long-term applications. A biomimetic approach was used to understand the functions and mechanisms of materials found in nature. Referred to as a biologically inspired design, adaptation, or derivation from nature, biomimetics was derived from ancient Greek words "biomimesis;" "bio" means life and "mimesis" means imitate and permits one to mimic biological structures and develop materials, devices, structures, and processes inspired by nature.[3]

An example of a widely used biomimetic concept is plant-inspired structures. Plants have been considered a source of inspiration for several years. Initially, structures such as trichome surfaces and rinds of fruits were mimicked. Beyond macrostructures, plants have become promising contenders in providing eco-friendly constituents that are converted into a broad range of nanomaterials, nanodevices, and nanostructures inspired by micro–nanoprocessing systems. Through several techniques, primary plant ingredients, such as cellulose, hemicellulose, and lignin, can be derived into nanocellulose, nanohemicellulose, and nanolignins with divergent and controllable properties. Nontoxic metals and metal oxides can also be obtained by utilizing minor plant components, such as essential oils with high bioavailability, biocompatibility, and bioactivity.[4] Nontoxic chemical constituents of plants help eliminate or minimize harmful and polluting substances during nanomaterial synthesis. In addition, bioactive and biodegradable compounds obtained from medicinal herbs are effective as an anticancer (taxol) and treating liver disease (silymarin).[5] Natural substances from plants not only produce zero pollutants but also completely decompose. Particularly, natural-origin compounds are readily available and do not require special chemical synthesis processes. Their composition and chemical structure make them promising sources of natural substances.[6]

As shown in **Figure 1**, plants have micro–nanosystems that inspired the development of nanomaterials, from the surface level to the molecular level. Osmotic actuation of plant cells can make plants responsive and adaptable to the surrounding environment. Plants are built from structures that can survive and regenerate faster than other organisms, enabling them to withstand predators and extreme weather owing to their sessility.

R. Luthfikasari, T. V. Patil, S. D. Dutta, K. Ganguly, M. M. Espinal, K.-T. Lim
Department of Biosystems Engineering
Kangwon National University
Chuncheon 24341, Republic of Korea
E-mail: ktlim@kangwon.ac.kr
T. V. Patil, K.-T. Lim
Interdisiplinary Program in Smart Agriculture
Kangwon National University
Chuncheon 24341, Republic of Korea
D. K. Patel, K.-T. Lim
Institute of Forest Science
Kangwon National University
Chuncheon 24341, Republic of Korea
The ORCID identification number(s) for the author(s) of this article can be found under https://doi.org/10.1002/smll.202201417.

DOI: 10.1002/smll.202201417

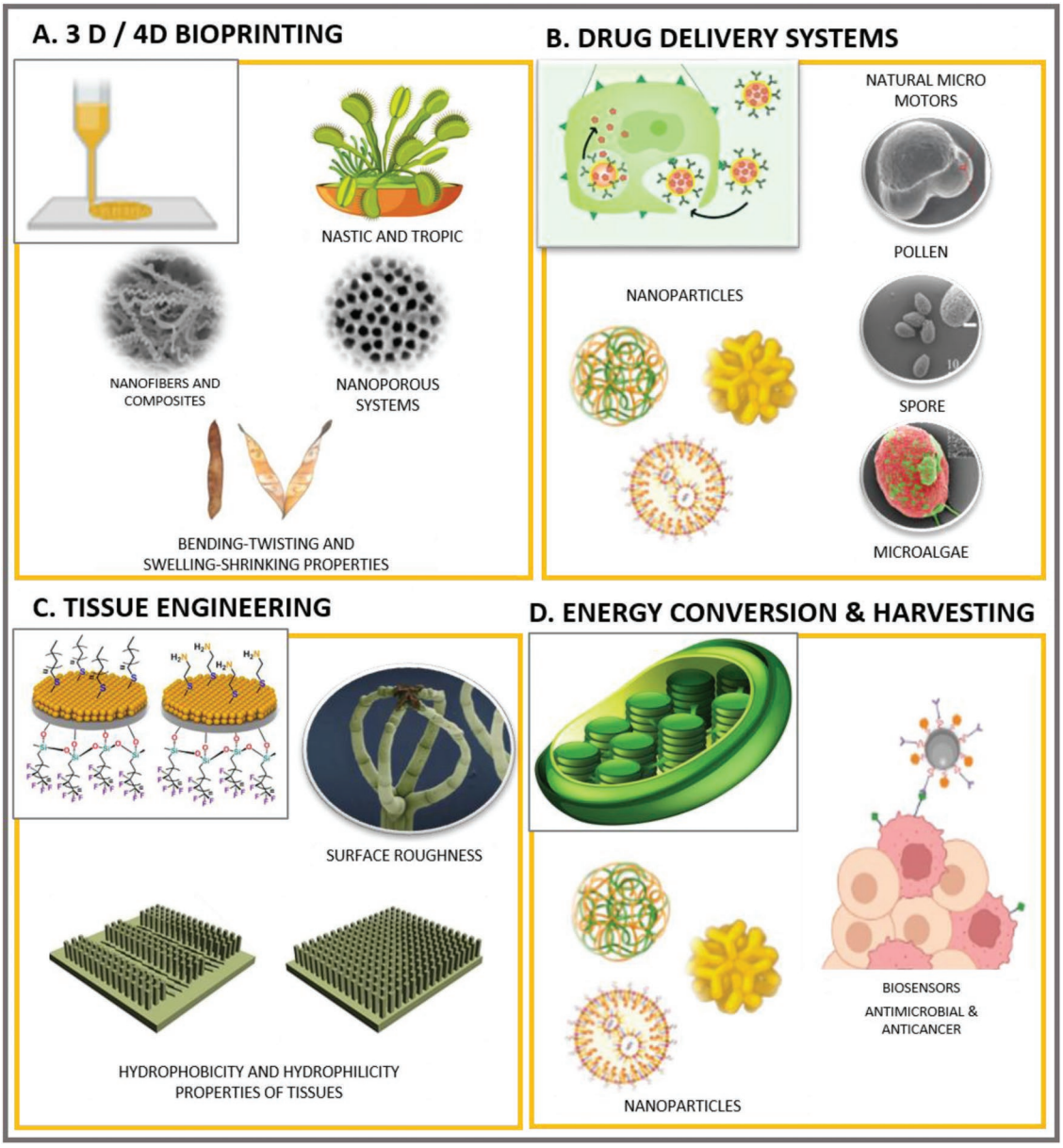

Figure 1. Classification scheme of micro–nano concepts and materials derived and inspired from plants and their biomedical application. A) Nastic and tropic movement contributes to bending–twisting and swelling–shrinking properties on plants influenced by osmotic actuation systems. Reproduced with permission.[8] Copyright 2018, MDPI. Reproduced under the terms of the CC-BY license.[13] Copyright 2015, Macmillan Publishers Limited. B) Natural micromotors contributed to drug delivery systems. Reproduced with permission.[9–12] Copyright 2004 and 2019, The American Association for The Advancement of Science. Copyright 2019, RSC Publishing. Copyright 2021, American Chemical Society. C) Plant's unique surface roughness properties inspire hydrophobicity and hydrophilicity properties of tissues. Reproduced under the terms of the CC-BY license.[13] Copyright 2015, Macmillan Publishers Limited. Reproduced with permission.[14,15] Copyright 2017, Springer Nature. Copyright 2019, Wiley. D) Inspiration from the plant's energy conversion and harvesting properties utilizing nanoparticles and adapted into biosensors with antibacterial activity.

Minimal specializations of tissues and cells and well-organized sensing systems that can receive abiotic and biotic signals are built from cells. These movements are actuated by rapid chemical reactions, and osmotic pressure differences allow plants to react rapidly to potential threats with appropriate responses (e.g., nastic and tropic movements), as shown in Figure 1A.[7] Plants also exhibit plasticity in their morphology and physiology to adapt to variability within their environment, which has high sensitivity, responsiveness, and tolerance to chemical substances and physical properties affected by the environment. This characteristic indicates that plants have higher adaptation and flexible interactions with unpredictable weather conditions and extreme environments.[3] Pollen and spore production can withstand these environments; they are the most suitable natural micromotors for delivering genetic materials (Figure 1B). The surface roughness of plant cuticles inspired superhydrophilic and superhydrophobic materials, as shown in Figure 1C. Furthermore, plants were also used as inspiration for energy

conversion and harvesting because of their ability to transform energy of sunlight into chemically produced organic energy and store it in the form of carbon through photosynthesis (Figure 1D).

Plants are sources of renewable materials, such as wood, resins, oils, and dyes for agro-based industries. The production of plants-based biofuels, like sugarcane and jatropha, are one of the alternative potentials to fossil fuels. In addition to their commercial worth, plants are beneficial because plants absorb CO_2 and clean the atmosphere, water, and soil by absorbing significant amounts of CO_2 and heavy metals. In addition, plant nanostructures have exhibited significant potential for micro–nanorobot development.[5]

Plants have different operations to humans and animals. However, this does not limit biomimetic adaptations to be used as inspiration across fields of science. Plant-based and plant-derived materials are essential for building a plant-actuated micro–nanorobot platform that is safe, sustainable, efficient, eco-friendly, and highly biocompatible and can be produced and operated cost-effectively. These traits are advantageous for biomimetic technologies derived from plants at the micro- and nanoscale across several fields, including biomedicine. Here, we present a comprehensive overview summarizing plant-actuated micro–nanorobots, including micro–nanostructures and systems on plants that can be adapted strategically through a biomimetic approach into emerging novel plant-actuated micro–nanoengineered materials for biomedical applications via the micro–nanorobot platform. Furthermore, we discuss how micro–nanostructures (e.g., nanoparticles, nanofibers and their composites, nanoporous materials, and natural micromotors) derived from plants are adapted into emerging biomimetic biomaterials. We also investigate how micro–nanosystem properties of plants, e.g., surface roughness, osmotically induced movements (nastic and tropic), and energy conversion and harvesting that are unique to plants, can further become sources of inspiration for biomimetic studies. The promising and challenging aspects following the implementation of various organisms and fields are also addressed to provide better adaptation of plant-actuated micro–nanorobot platforms in the future, particularly in the biomedical field.

2. Biomimetic Approach

Biomimetics is more complex than can be derived from its origins. Understanding natural phenomena and the principles underlying their mechanisms is complex and challenging. Several branches of science struggle to obtain maximum potential from nature and apply the concepts that may give advantages to science, engineering, and particularly biomedical aspects.[16]

Knowledge and competencies are essential for understanding and applying biomimetics. Experts from various scientific fields have systematically analyzed and transferred biological insights into technical applications through an interdisciplinary approach. Stepwise processes were used to develop biomimetic products. **Figure 2** shows a schematic of the differences between the biology push process (i.e., bottom-up approach), from the biological research question, and the technological pull process (i.e., top-down approach), which begins by formulating a technical challenge. After selecting a suitable biological model, the next step is to decipher and translate the functional principles into an engineering-compatible language.[17]

The bottom-up biomimetic approach begins with a promising result of a fundamental biological model that is further implemented in technical aspects. The initial step is to analyze the biomechanical elements and functional morphology, followed by quantitative analysis to better understand applicable structures, shapes, and functions. The next step is to separate the obtained principles from the biological model to create a new, original model. Abstraction and detachment are the most important and challenging processes in biomimetic projects

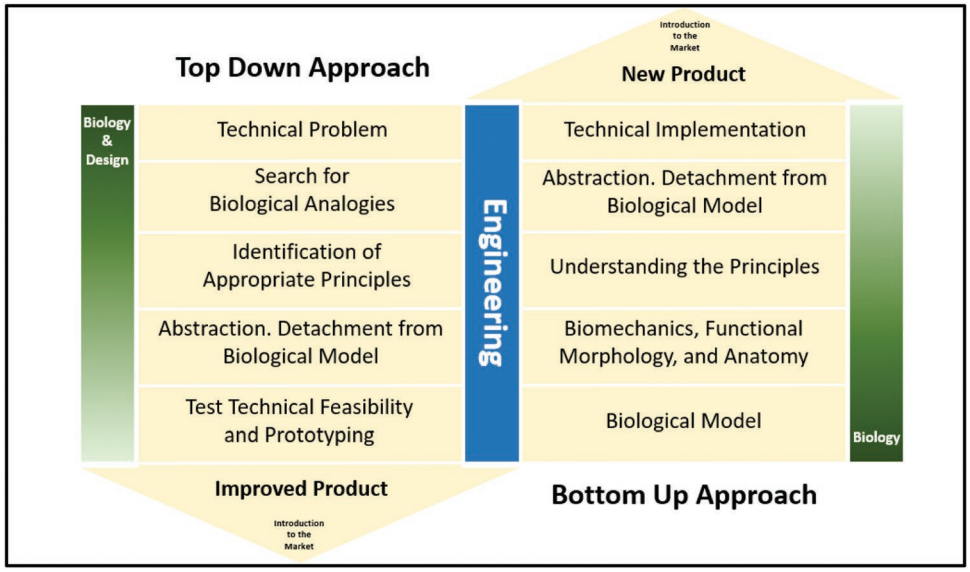

Figure 2. The biomimetic schematic approach used for adapting biological design into engineering application. Adapted with permission.[18] Copyright 2008, WIT Press.

to develop novel technical aspects. Successfully developed technical applications must be well understood by the project partner from other experts in nonbiological fields, and the technical implementation in the laboratory and in engineering can be analyzed for potential industrial establishment. The entire biomimetic process not only depends on biologists and engineers but also forms a continuum in cooperation with other scientific and industrial partners and has to pass through several iterative loops to obtain interim results.[18]

Through the top-down approach, biomimetics is sought to improve and develop innovations in already existing specialized products that might have previously been established in the market. For a successful top-down process, expertise from engineers and biologists is required to improve and develop an existing product as the center of cooperation. The first way to start the top-down process begins with an identification of technical problem. Its boundary conditions must be exactly defined so that biologists can find promising solutions to solve a technical problem. Several biological templates are required to render screening processes that suitable as concept provide on specific technical requirements. The results were then selected for deeper analysis, experimental exploration, and characterized based on their compatibility for the problem.[18]

3. Types of Micro–Nanostructures

3.1. Nanoparticles

There are several methods of synthesizing nanoparticles, which have been applied physically, chemically, and biosynthetically to improve the synthesis efficiency. There are three principal parameters for the green synthesis of nanoparticles. One is selecting a green or environmentally friendly solvent, second is choosing high quality of the reducing agent, and third is using a nontoxic stabilizing material. Typically, chemical methods are expensive when using toxic hazardous chemicals. These methods are responsible for various environmental risks.[19] Therefore, safer, highly biocompatible, and eco-friendly routes are preferred for synthesizing nanoparticles by consuming plants and microorganisms for biomedical applications.[20]

Phyto-nanotechnology has emerging potential to produce different nanoparticles by employing extracts from different parts of plants (e.g., leaves, fruits, roots, stems, and seeds),[21] and their phytochemicals act as a stabilizer and reducing agent.[22] Therefore, there has been significant development of greener routes to prepare nanoparticles as the demand increases. The three current green methods are plant molecular farming;[21] green synthesis of silver nanoparticles by using plant extracts, enzymes, bacteria, biodegradable polymers, and microwaves;[23] and gold nanostructures at room temperature using biodegradable plant surfactants.[24]

Plant molecular farming uses in vitro cultured tissues of the entire plant as a synthesizer of desirable recombinant proteins and is economically feasible to be cultured in large-scale bioreactors. Plants have already proven to be an outstanding alternative to phytomaterials and biomaterials through the exogenous and endogenous synthesis of nanoparticles. Therefore, this technique provides a solution for the production of metallic nanoparticles and therapeutic proteins (e.g., elastin, gelatin, collagen, recombinant anticancer monoclonal antibodies, and vaccines using green factories).[21]

Nadagouda et al. in 2009 developed a green synthesis of gold nanostructures at room temperature using VeruSOL-3, a naturally occurring plant surfactant mixed with p-limonene, and VeruSOL-10, VeruSOL-11, and VeruSOL-12, which are individual plant-based capping agents free surfactants derived from castor oils and coconut. These techniques enable fine-tuning of materials in response to various stimuli (e.g., magnetic, electrical, optical, and mechanical stimuli).[24] Furthermore, greener techniques were developed by Hebbalalu et al. in 2013 for the synthesis of silver nanoparticles using polyphenols or plant-based sugar, biodegradable polymers, bacteria, and enzymes with energy sources from microwaves under ambient conditions. However, in addition to proven benefits, there remain inherent safety concerns regarding degradability and movement that depend on the coating used and must be followed by toxicological tests.[23]

Numerous biological and physicochemical routes of nanoparticle synthesis are divided under two discrete classes, as shown in **Figure 3**A. The first class uses the bottom-up approach, which generates nanoparticles through the self-assembly of atoms into new nuclei or smaller units, such as molecules and atoms. They possess nanoscopic dimensions that grow into particles, which can be employed in various chemical and biological methods. The second class uses a top-down approach, in which nanoparticles are formed by the size of the reduction method, i.e., a suitable bulk material is reduced into small units using appropriate lithographic techniques.[25] The use of sacrificial templates, block copolymers, and biomolecules (DNA, protein, and enzymes) has also been reported as green synthesis routes for nanomaterials. The synthesis strategy summary and basic growth mechanism of nanoparticle synthesis using plant extracts are shown in Figure 3B. The antifungal activity mechanism of TiO_2 nanoparticles toward selected pathogens, including *Aspergillus fumigatus, Arthrographis cuboid*, and *Aspergillus niger*, is shown in Figure 3C. The results of antifungal activity in Figure 3D,E indicate that nanoparticles have effective antibacterial properties at specific dosages at various temperatures and pH values.[26]

Nanoparticles can be synthesized from thoroughly washed and sterilized flowers, roots, tubers, and plant leaves, followed by drying at room temperature. The weight of the dried samples was measured and crushed. The powder was then mixed with Milli-Q H_2O at the desired concentration and boiled with continuous stirring. The obtained solution was filtered, and the clear portion was used as the sample.[27] **Table 1** shows plant-assisted synthetic nanoparticles and their various roles in biomedical applications.

3.2. Nanofibers and their Composites

Cellulose has notable biomedical properties, including biocompatibility, low cytotoxicity, outstanding mechanical properties, superior chemical stability, and cost-effective. Excellent physicochemical properties can be obtained by tuning cellulose at the micro- and nanoscale. Therefore, cellulose nanocomposite has promising applications in biomedical, such as wound healing,

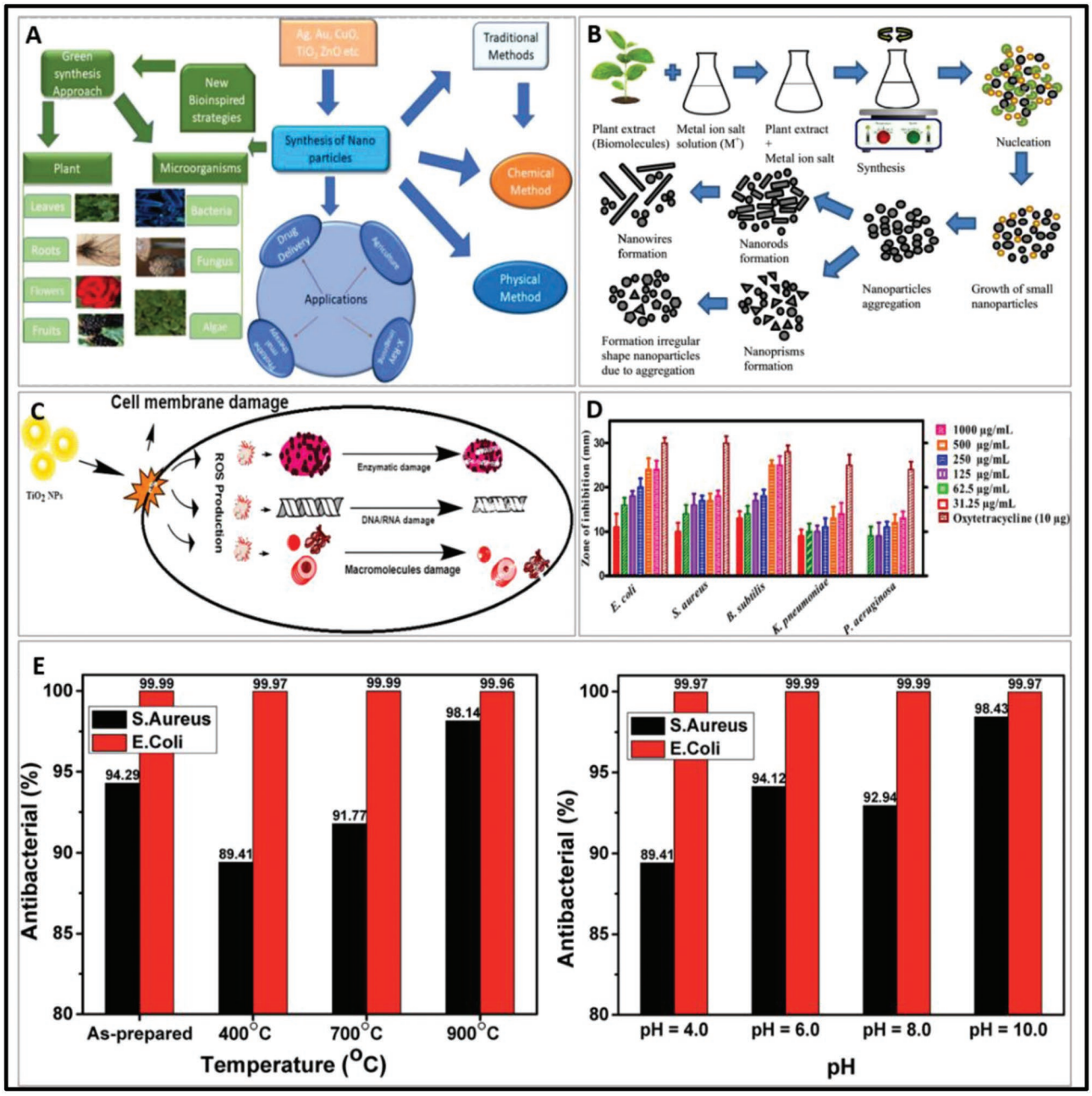

Figure 3. A) Flow chart of general synthesis of green nanoparticles and their applications. Reproduced with permission.[26] Copyright 2021, Elsevier. B) The mechanism of nanoparticles synthesis using plant extract. Reproduced with permission.[28] Copyright 2014, IOP Publishing. C) Mechanism of antifungal reaction of Green synthesis of TiO_2 nanoparticles. Reproduced under the terms of the CC-BY license.[29] Copyright 2018, Informa UK Limited (Taylor and Francis Group). D) Antibacterial activities of ZnO nanoparticles. Reproduced with permission.[30] Copyright 2019, Elsevier. E) The ZnO NPs bactericidal rates toward *Escherichia coli* and *Staphylococcus aureus* at various annealing temperatures and different pH values. Reproduced with permission.[31] Copyright 2020, RSC Publishing.

tissue engineering, 3D printing, drug delivery, and medical implants. Cellulose is the basic component of plant fibers and is enclosed by lignin and hemicellulose. Cellulose chains are arranged as fibrils in the plant cell wall, which assembled into microfibrils with a few nanometers of diameters. Top-down approaches have been used for the conversion of cellulose to various macro- and nanoscale materials.[66] The most used nanocelluloses are cellulose nanofibers (CNFs) and cellulose nanocrystals (CNCs), which have high strength and high surface area, and are isolated from cellulose fibers by mechanical fibrillation and acid hydrolysis, respectively.[67] High-pressure homogenization, grinding, ultrasonication, and refining methods can also be used to isolate CNFs.[68] CNFs and CNCs have different dimensions; CNF has an interlinked network of fibers 2–5 mm in length,[67] colloidally stable with diameters of 5–50 nm and a few micrometers, containing more crystalline material.[66]

Table 1. Plant extract-assisted nanoparticles synthesis.

NP	Plant	Part of plant	Precursor	Application	Ref.
Ag	*Tagetes erecta*	Flower	$AgNO_3$	Photodegradation of rhb dye	[32]
	Diospyros malabarica	Fruit	$AgNO_3$	Antimicrobial, anticancer, and catalytic reduction of 4-nitrophenol (4-NP)	[33]
	Morinda citrifolia	Leaf, pulp, seed	$AgNO_3$	Antibacterial activity	[34]
	Annona muricata	Peel	$AgNO_3$	Inducer of apoptosis in cancer cells and inhibitor for NLRP3 inflammasome via enhanced autophagy	[35]
Ag-Fe	*Tamarindus indica*	Shell	$AgNO_3$, rGO, FeNP	Photocatalytic degradation of toxic dyes	[36]
	Salvia officinalis	Leaf	$AgNO_3$ and $Fe(NO_3)_3$	Catalytic capability for 4-nitrophenol reduction	[37]
	Beta vulgaris	Root	$AgNO_3$ and $Fe(NO_3)_3$	Antifungal agents	[38]
	Gardenia jasminoides	Leaf	$AgNO_3$ and $Fe(NO_3)_3$	Synergistic combinatorial antimicrobials activity	[39]
Au	*Gelidium pusillum*	Leaf	$HAuCl_4$	Anticancer activity	[40]
	Hibiscus sabdariffa	Flower	$HAuCl_4$	Antiacute myeloid leukemia	[41]
	Pimenta dioica	Leaf	$HAuCl_4$	Anticancer activity	[42]
	Croton sparsiflorus	Leaf	$HAuCl_4$	UV-protection, antibacterial, and anticancer agents	[43]
Au-Ag	*Trapa natans*	Peel	$AgNO_3$ and $HAuCl_4$	Cancer therapy	[44]
	Madhuca longifolia	Seed	$AgNO_3$ and $HAuCl_4$	Enhancement in wound healing bio-efficacy	[45]
	Citrus sinensis	Peel	$AgNO_3$ and $HAuCl_4$	Electrochemical determination of caffeine	[46]
	Rumex hymenosepalus	Root	$AgNO_3$ and $HAuCl_4$	Antimicrobial agents	[47]
Cu	*Vaccinium myrtillus*	Fruit	$CuCl_2$, $Cu(CH_3COO)_2$ $Cu(NO_3)_2$	Antimicrobial activity	[48]
	Citrus limon	Fruit	$CuSO_4{\cdot}5H_2O$	Antibacterial activity	[49]
	Cissus arnotiana	Leaf	$CuSO_4$	Antioxidant and antibacterial activity	[50]
	Allium eriophyllum	Leaf	$CuSO_4$	Antimicrobial and cutaneous wound-healing potential	[51]
CuO	*Allium sativum*	Bulb	$Cu(NO_3)_2$	Antimicrobial, antioxidant, antilarvicidal activities	[52]
	Annona muricata	Leaf	$CuSO_4{\cdot}5H_2O$	Enhanced photocatalytic performance	[53]
	Azadirachta indica	Leaf	$CuSO_4$	Induce apoptosis against cancer cells	[54]
	Beta vulgaris	Root	$CuSO_4{\cdot}5H_2O$	Antibacterial and anticancer activities	[55]
Pd	*Peganum harmala*	*Seed*	$Pd(OAc)_2$	*Antitumor activity, antioxidant activity, antineoplastic agents*	[56]
	Couroupita guianensis	Whole-body	$Pd\ Cl_2$	Antibacterial and cytotoxicity effects	[57]
	Solanum nigurum	Leaf	$Pd\ Cl_2$	Antimicrobial and catalytic activities	[58]
	Diospyros kaki	Leaf	$Pd\ Cl_2$	Antibacterial activity	[59]
Pt	*Ononidis radix*	-	K_2PtCl_6	Anticancer activities	[60]
	Tragia involucrata	Leaf	$H_2PtCl_6{\cdot}6H_2O$	Antioxidant, antibacterial, and mitochondria-associated apoptosis in HeLa cells	[61]
	Peganum harmala	Seed	$PtCl_4$	Antitumor activity, antioxidant activity, antineoplastic agents	[56]
	Phoenix dactylifera	Fruit	H_2PtCl_6	Toxic and protective effects in ccl4 induced hepatotoxicity	[62]
TiO_2	*Withania somnifera*, *Eclipta prostrata*, *Glycyrrhiza glabra*	Root	$Ti[OCH(CH_3)_2]_4$	Anticancer and antibacterial applications	[63]
ZnO	*Artocarpus heterophyllus*	Leaf	$Zn\ (NO_3){\cdot}6H_2O)$	Anticancer and apoptotic activity	[64]
SnO_2	*Parkia speciosa*	Pods	$SnCl_4{\cdot}5H_2O$	Antioxidant and photocatalytic properties	[65]

The high aspect ratio of CNF resulting in shear thinning and thixotropic behavior.[69,70] Shorter CNC typically measures a few hundred nanometers in length.[66,67] Cellulose nanowhiskers (CNWs) are needle-like or rigid rod-like nanowhiskers with a width of 5–70 nm and length of 200–500 nm with a sulfate group at the surface. The morphology depends on the cellulose source and the characteristic properties of CNWs have high aspect ratio, superior strength, poor thermal expansion, wide specific surface area, outstanding bending strength, low density, and self-assembly in liquids.[71,72] CNWs have applications as emulsifiers, fillers, stabilizers, and thickeners in the food and pharmaceutical industries.[66,73] Nanofibers and nanocrystals have been extracted from wood, rice straw, wheat straw, bagasse, banana, pineapple leaf, and cotton. Although there are

limited studies on the use of CNF as reinforcements, existing studies suggest that nanofibers have the potential to disperse homogenously in matrices.[74] However, advanced polymer materials can show special functions accordance to external conditions. More scientifically, this behavior is similar to the biological intelligence observed in nature, termed smart polymers or stimuli-responsive polymers.[75] There are three types of smart polymer: 1) shape memory intelligent polymers (SMPs), which can transform their shape in a predefined method from two different shapes under an appropriate stimulus;[76] 2) shape-healing polymers that are able to convert energy to repair damage autonomously or nonautonomously under external force without any involvement from humans to regain the initial properties;[77] and 3) responsive polymers, which are triggered by stimuli from external, including temperature, light, electrical and magnetic fields, and chemicals.[78]

Cellulose crystallites, cellulose nanocrystals, microcrystalline cellulose, and hydrolyzed starch are the crystalline components of starch obtained via hydrolysis to different extents.[79] Initial research on cellulose nanocrystals was initiated by Dufresne et al. in 1996, who performed an acidic hydrolysis method to isolate microcrystalline cellulose with diameters of approximately a few tens of nanometers.[80] Putaux et al. in 2003 extracted nanocrystals from waxy maize starch sizes between 15 and 40 nm in both diameter and length using the acid hydrolysis method.[81] Recently, cellulose nanocrystals isolated from potatoes,[82–84] peas,[85,86] and waxy maize[87–89] have been reported with various diameters in the range of 40–150 nm. This variation is thought to be because of the source of starch and its botanical origin.[90] Cellulose nanofibrils and nanocrystals can be isolated from pure rice straw cellulose by sulfuric acid hydrolysis, mechanical blending, and 2,2,6,6-tetramethylpiperidine-1-oxyl (TEMPO)-mediated oxidation.[91] The TEMPO-mediated oxidation procedure is interesting because it produces the finest and most uniform nanofibers with a diameter of ≈1.7 nm; however, it produces the lowest crystallinity. A strong acid such as sulfuric acid is typically used for cellulose hydrolysis, which is immediately followed by quenching with deionized water. To achieve higher cellulose concentrations, the suspension was centrifuged and the extra aqueous acidic solution was removed. The isolation of starch nanocrystals includes two prevailing processes, starch type and origin are negligible and both of are based on the acidic hydrolysis method. The first method, demonstrated by Dufresne et al. in 1996, included hydrolysis using hydrogen chloride, whereas the second method, described by Angellier et al. in 2004, used sulfuric acid.[87] Kaushik et al. in 2015 reported cellulose nanocrystals with a severely high concentration of Pd nanoparticles deposited in enantiomeric chirals as catalysts for the hydrogenation of prochiral ketones in water at room temperature.[92] These cellulose nanocrystals acted as the supporter and chiral source and delivered 65% Pd nanoparticle deposits, providing insight into the chiral induction mechanism.[93]

3.3. Nanoporous Systems

Nanoporous materials consist of organic or inorganic frameworks that support stable porous structures derived from various natural plants. They were fabricated using a simple, cost-effective, and efficient ways.[94,95] To develop high-performance energy storage devices that can meet sustainable requirements, various energy devices, such as electrical double-layer capacitors, use carbon as the main active compound for electrodes. Carbon materials provide high conductivity and stability, cost-effectiveness, and efficient design. Therefore, the development of sustainable energy-storage devices with high conductivity depends significantly on the electrode materials used to produce activated carbon electrodes derived from plant biomass.[95] Chen et al. in 2014 developed novel nitrogen-doped nanoporous carbon nanosheets derived from *Typha orientalis*. These high surface area nanosheets have abundant micropores and a high nitrogen content for an efficient oxygen reduction reaction (ORR).[94] The ORR is a vital reaction in life- and energy-converting system processes, such as biological respiration, fuel cells, and metal-air batteries.[96] The developed nitrogen-doped nanoporous carbon nanosheets exhibited similar catalytic activity in alkaline media, with the methanol tolerance level being higher than that of commercial 20% platinum on carbon (Pt/C). Additionally, it provides a simple method to synthesize excellent electrocatalysts, which is a low-cost, simple, and readily scalable approach, because it is directly derived from biomass. These broad applications are expected to be applied in the fields of supercapacitors, lithium-ion batteries, biosensors, gas uptake, and removal of pollutants[94] from biomedical device residues.

The fabrication process of the nanoporous carbon nanosheets (NCSs) is shown in **Figure 4**A. The flower spikes (b) of the *T. orientalis* plant (a) were collected, and the raw material (c) was processed under a hydrothermal process at 180 °C for 12 h to form a carbonaceous hydrogel (d). By freeze drying the hydrogel, NCS aerogel was obtained and annealed in an NH_3 atmosphere at 800 °C for 2 h at a heating rate of 5 °C min^{-1} and then cooled at a rate of 5 °C min^{-1}, after which (f) NCS-800 was obtained. Figure 4B-a–c shows representative scanning electron microscope (SEM), scanning transmission electron microscope (STEM), and high-resolution transmission electron microscope (HR-TEM) images of NCS-800. Elemental mapping of the nanosheets (Figure 4B-d–f) indicates that the products contain carbon, oxygen, and nitrogen. Figure 4C summarizes the proposed formation mechanism of the NCS-800.[94]

3.4. Micro–Nanomotors

Micro- and nanorobots are micro- and nanometer-scale devices that are beneficial to several fields, including the biomedical field. Their size became a particular benefit of these devices in healthcare, as it assists with minor invasive procedures of surgery and nontargeted therapies using chemicals and radiation.[97] Various dynamic biological motors are available in nature, such as kinesins, dyneins, sperms, and certain bacteria that can convert energy from the physiological environment to mechanical force. Therefore, natural motors can efficiently perform autonomous motions and complex tasks. Therefore, artificial micro–nanomotors have been developed based on these natural motors. Self-propelled and fuel-based synthetic micro–nanomotors are well-propelled in diverse fluids. They

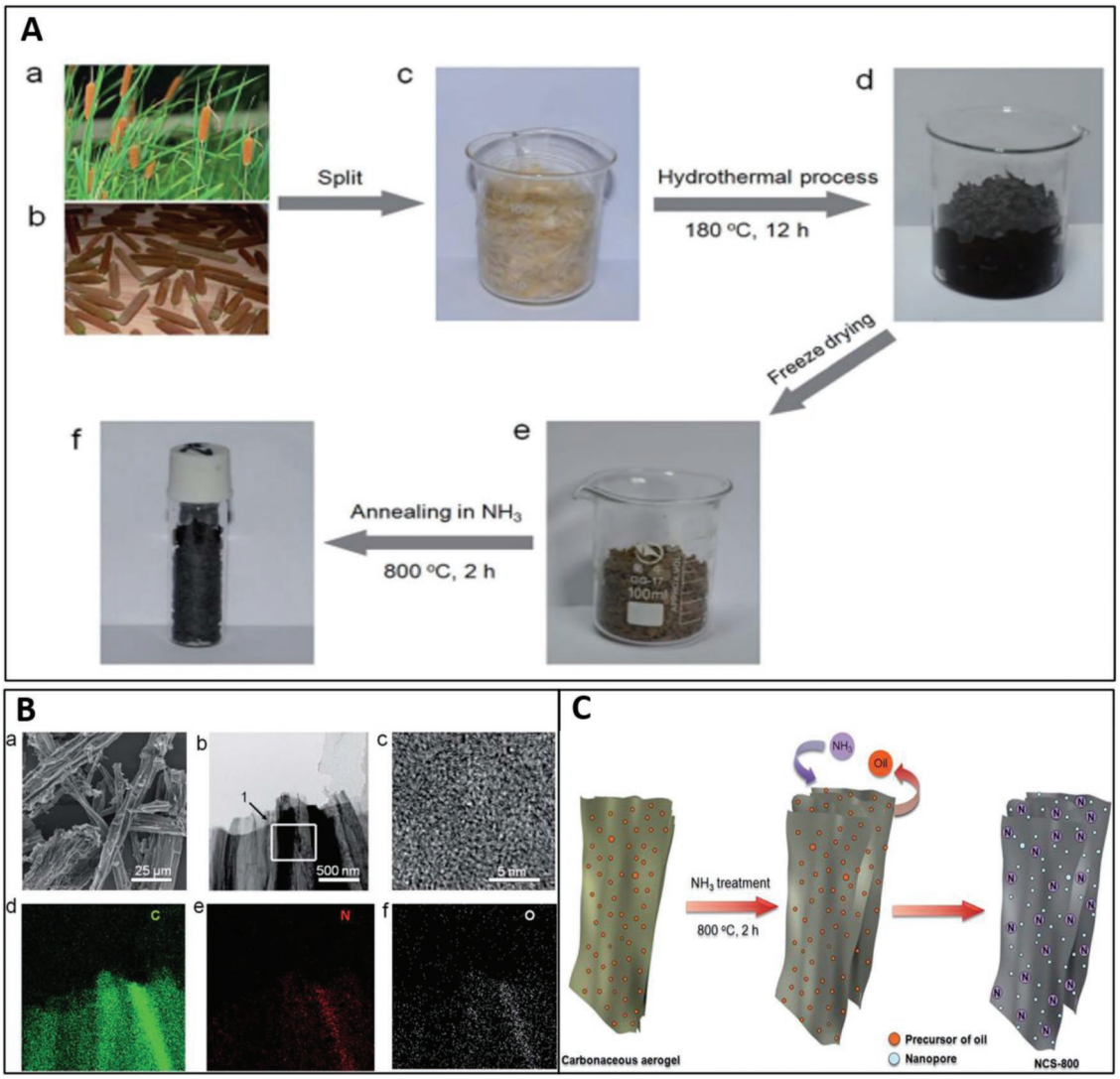

Figure 4. A) Nitrogen-doped nanoporous carbon nanosheets derived from plant biomass preparation steps. a) Images of *Typha orientalis*, b) flower spikes, c) raw material for hydrothermal process, d) carbonaceous hydrogel, e) carbonaceous aerogel, and f) product NCS-800. B) a–c) SEM, STEM, and HR-TEM images of the NCS-800; d–f) carbon, nitrogen, and oxygen element mapping. C) Proposed formation mechanism of the NCS-800. Reproduced with permission.[94] Copyright 2014, RSC Publishing.

can complete various tasks that passive devices cannot, such as penetration of specific cells and tissues.[98] Therefore, these systems showed more practical applications in vitro and in vivo, exhibiting promising potential in biomedical applications, such as drug delivery,[99,100] biosensing,[101] cancer therapy,[102] imaging,[103] assisted fertilization,[104] and precision micro–nanosurgery.[105] However, until recently, most of the micro–nanomotors were chemically driven by hydrogen peroxide,[106] which causes oxidative toxicity and is unsuitable for biomedical applications. Therefore, there is a growing need to conduct research on micro–nanomotors using a biocompatible fuel as a power source, such as glucose, urea, water, a combination of magnesium with water, ionic zinc with gastric acid, and several external force-induced powers (e.g., magnetic fields, ultrasound waves, and light sources).[107]

Most of the framework materials of micro–nanomotors have issues regarding biodegradability and compatibility. Consequently, the body recognizes these synthetic micro–nanomotors as harmful substances that may induce immune responses or inflammation.[108] Several approaches have been employed to improve biocompatibility and biodegradability, such as the use of novel framework materials, fuel sources, and biological components. Using eco-friendly sources for the motor, such as pollen, spores, and microalgae, is an attempt to increase the rate of biocompatibility and biodegradability.

Pollen grains and plant spores have emerged as materials with multiple applications in drug and vaccine delivery, removal of heavy metals, and as catalyst supports. Natural pollen and spore microcapsules act as a shell protecting genetic material from external impairment, mostly comprising the sporopollenin and intine layers. The hollow sporopollenin exine shells provide some notable features, such as homogenous size, nontoxic nature, high resistance to alkalis and acids, and ability to withstand elevated temperatures, which are beneficial

for microencapsulation and controlled drug delivery and release.[109]

Their examples and properties are presented in **Table 2**.[107]

Pine pollen is widely distributed in nature and has unique three-cavity structure consists of a central cavity containing cytoplasm and two cavities of air sacs. Sporopollenin biopolymers and lipids comprised most of the outer wall of pollen grains, and cellulose mainly composed the inner wall with several pores below 200 nm in size distributed on the outer wall of pine pollen. Sun et al. in 2019 developed pine pollen-based micromotors (PPBMs) by encapsulating magnetic particles and medicines via vacuum loading. PPBMs are highly efficient and inexpensive, with excellent permeability and renewability. The fabrication of the PPBMs is shown schematically in **Figure 5**A. Natural pine pollen has low permeability, mainly as a result of its outer lipid-suppressing liquid uptake. The first defatting technique is to dispose of contaminants and reduce surface-connected lipid compounds, ensuing in multisized pores that in the long run beautify and facilitate the loading of the compound. Defatted pine pollen changed into uncovered to a vacuum (0.01 mbar) for 15 min after thorough blending with the magnetic iron nanoparticles and the drug. In addition to maintaining a uniform size distribution and complete microstructure, the resultant PPBMs exhibited an excellent magnetic actuation capability. This contrast demonstrates that the defatting step does no harm to the unique microstructure. Morphological remark of the pollen surface changes by defatting via SEM shows that the degreasing technique effectively eliminates the lipid compounds attachment to the surface and exposes higher-density of nanopores at the air sacs cavity to facilitate encapsulation. The enlarged SEM images in Figure 5B show the presence of iron attributed to the magnetic nanoparticles (Fe_3O_4), and the magnetization curves are presented in Figure 5C. Figure 5D shows the successful inheritance of doxorubicin (DOX) through fluorescence microscopy. Propelled by the magnetic field, superimposed snapshots of moving PPBM illustrations on the tracking trajectories along predefined routes of a rectangle for rolling, triangle for spinning, and square for tumbling modes are shown in Figure 5E under the closed-loop control system for navigated locomotion, as illustrated in Figure 5F. The PPBMs then navigated the locomotion trajectories in fluorescence mode in distilled water along the predefined alphabet R, O, B, and T routes (Figure 5G).[12]

In addition to pollen, spores produced by a various plant and fungal species are common in nature. A complex 3D design of a spore's primary function is to protect sensitive genetic material from extreme environmental conditions. Moreover, each unique structure enables easy spreading and diffusion by various media, such as wind and water.[111] This natural 3D microarchitecture of spores is renewable and biocompatible with highly efficient and reproducible processes. These fascinating features make them attractive bio-templates for the development of novel functional materials for biomedical applications.[112,113] The preparation of fluorescent magnetic spore-based (spore@Fe_3O_4@CD) microrobots (FMSMs) includes a compound of facile chemical deposition, succeeding encapsulation, and functionalization strategies, as illustrated in **Figure 6**A. First, the pretreated *Ganoderma lucidum* spores have been magnetically encapsulated via way of means of a layer of Fe_3O_4 nanoparticles after chemical bath deposition under sealed ammonia conditions for 2 h. This process provides the FMSM with continuous remote magnetic propulsion, providing long-lasting propulsion with a variety of liquids. At room temperature, 3-mercaptopropionic acid in ethanol functionalized magnetic spores and attached to carbon dots through carbodiimide chemistry. They provided tracking availability and a novel capability to target *Clostridium difficile* toxins and biosensing functions by generating fluorescence quenching. The final form of FMSMs has a distinctive morphology, appropriate magnetic properties, exquisite red fluorescence, and selective targeting ability for real-time tracking owing to their fluorescence changes. Tracking is caused by the rotating magnetic field equipped with a fluorescence microscope and the rapid detection of toxins in practical samples. The SEM images of the original spores in Figure 6B show that the pollen had an oval shape with clear pores. Magnetic actuation for an FMSM includes spinning, rotation-translation, and tumbling. Here, B is the strength of the rotating magnetic field, f is the input frequency of the magnetic field, v is the translational velocity, denotes the rotation velocity, and the tilting angle between the rotation axes, and the direction angle is clearly illustrated in Figure 6C. The fluorescence motion trajectories of the FMSM in Figure 6D show the FMSM movement in distilled water

Table 2. Plant-derived micro–nanorobots and their properties.

Types	Power sources	Motion behaviors	Carriers/motors	Coating	Function	Ref.
Pollen-based micromotors	Rotating magnetic fields	Rolling, tumbling, spinning	Defatted pine pollen grain	Fe_3O_4	Anticancer drug Doxorubicin carrier and delivery	[12]
Spore-based micromotors	Rotating magnetic fields	Spinning, rotation-translation, and tumbling	Spore of *Ganoderma lucidum*	Fe_3O_4	Detect toxin of *Clostridium difficile* in patients' stools	[10]
Microalgae-based micromotors	2 motile flagella	Swimming	*Chlamydomonas reinhardtii*	Modified angiotensin-converting enzyme 2 (ACE2)	Binding and removal of S protein and SARS-CoV-2 virus	[11]
Microtubes	Rotating magnetic fields	Drilling	Calcified porous microneedles extracted from leaf of *Dracaena marginata*	Fe/Ti	Camptothecin anticancer drug carrier and delivery	[105]
Helical microswimmers	Rotating magnetic fields	Corkscrew motion	Spiral xylem vessel	Ti/Ni	Transporters	[110]

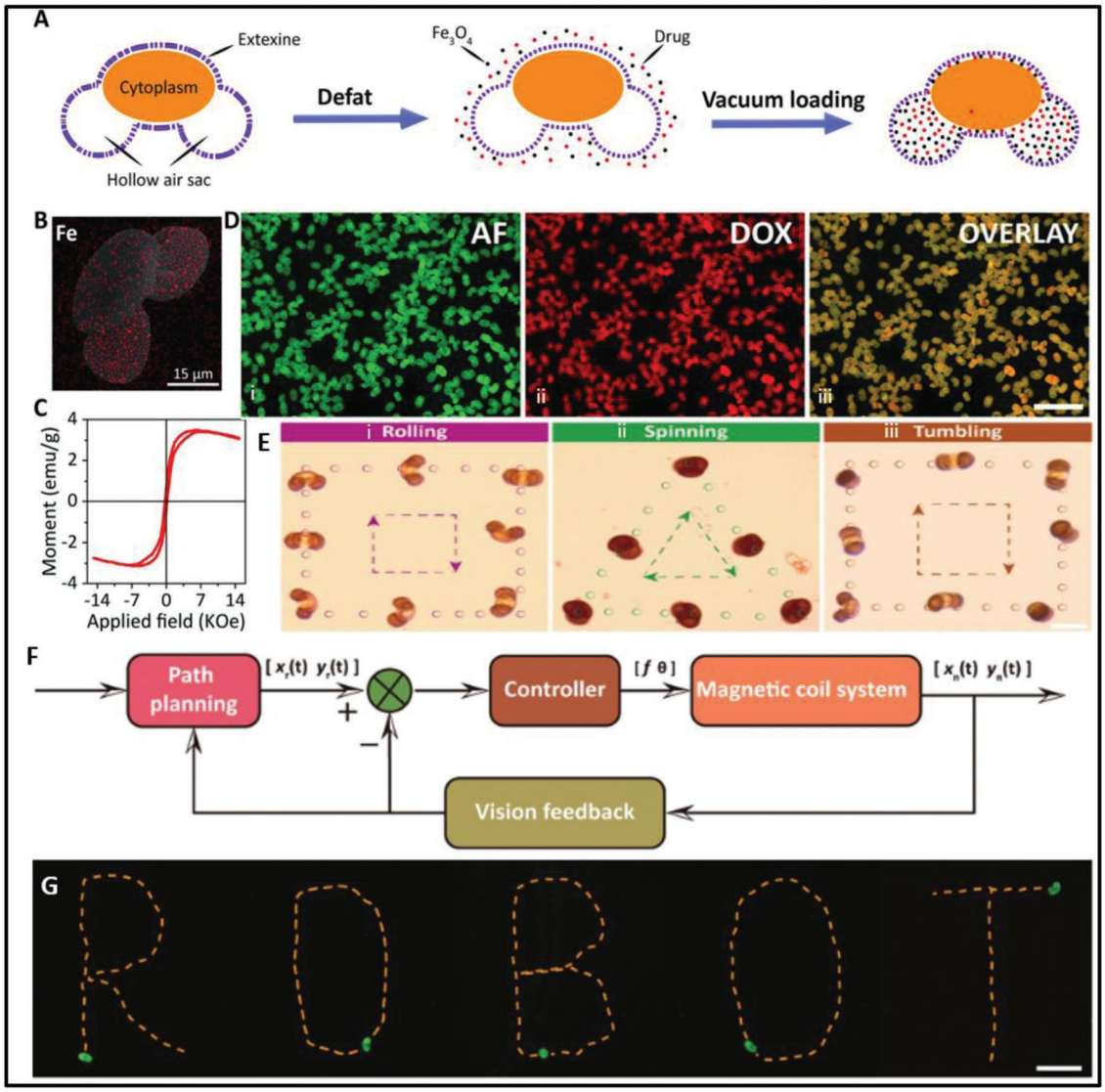

Figure 5. Fabrication and characterization of PPBMs. A) Schematic illustration of defatting and vacuum loading steps in the fabrication of PPBMs. B) The superimposed image of Fe attributed to the magnetic nanoparticles (Fe_3O_4) by using the energy dispersive X-ray analysis (EDX) map and the SEM. C) Magnetization curves of the prepared PPBMs. D) Fluorescent images of PPBMs loaded with anticancer drug doxorubicin (DOX). Scale bar, 200 μm. E) Illustration of the tracking trajectories along predefined rectangle, triangle, and square routes in the rolling, spinning, and tumbling modes, respectively. Scale bar: 50 μm. F) Closed-loop control system illustration for navigated locomotion. G) The locomotion trajectories of the PPBM in deionized water along the predefined alphabet R-, O-, B-, O-, and T routes in the fluorescence mode. Scale bar: 150 μm. Reproduced with permission.[12] Copyright 2019, RSC Publishing.

(DIW), phosphate buffered saline (PBS), Dulbecco's modified Eagle medium (DMEM), fetal bovine serum (FBS), mucus, and intestinal mucus (Imucus) in a rotating magnetic field. Automated FMSM motion was also tested by visualizing various fluorescence trajectories in DIW (Figure 6E).[10]

Algae can be referred to as plant-like organisms that use carbon dioxide (CO_2) to produce energy via photosynthesis, similar to autotrophic organisms, such as plants.[114] Algae have recently been used for wastewater treatment, but have not been used as active microrobots or to combat highly infectious viruses such as water contaminated with SARS-CoV-2. *Chlamydomonas reinhardtii* was selected as model algae because of its attractive properties such as long life span, fast locomotion in various aqueous environments, easy large-scale production, and facile surface functionalization. Zhang et al. in 2021 developed angiotensin-converting enzyme 2 (ACE2) receptors that were conjugated on the algal surface using a click chemistry approach (**Figure 7**A,B). Specifically, the azide and dibenzocyclooctyne (DBCO) groups via the *N*-hydroxysuccinimide ester reaction were conjugated into the ACE2 receptors and the algae. The conjugated N_3 on the ACE2 receptors then reacts with the DBCO on the algae effectively and forms an ACE2-algae robot. Immunostaining using Fluor488-conjugated anti-ACE2 antibody label on the green fluorescent protein (GFP) channel and Cy5 channel was carried out to envisage the ACE2 receptors successfully embed to the algae

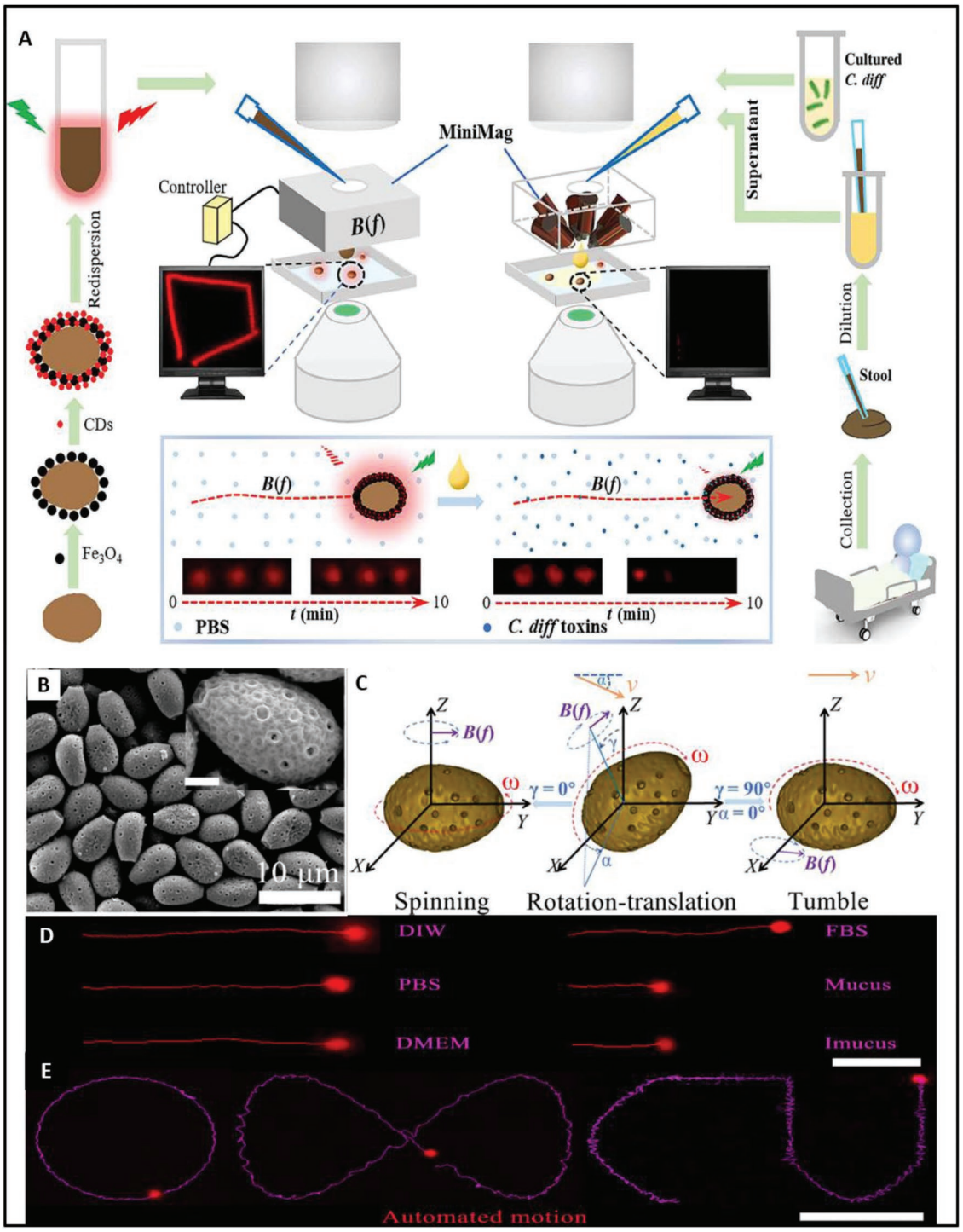

Figure 6. A) Preparation and potential application of FMSMs. The acquired FMSMs can carry out controlled locomotion in predefined tracks by observing the fluorescence change when BY being continuously driven in a rotating magnetic field. Swimming and fluorescence performance of FMSMs. B) SEM images of the original spores. C) Magnetic actuation of FMSM. D) Fluorescence motion routes of the FMSM in DIW, PBS, DMEM, FBS, mucus, and intestinal mucus (Imucus) under rotating magnetic field. E) Fluorescence routes of autonomous navigation of the FMSM in distilled water. From ref. [10]. Copyright Zhang et al., some rights reserved; exclusive licensee AAAS. Distributed under a CC BY-NC 4.0 license http://creativecommons.org/licenses/bync/4.0/. Reprinted with permission from AAAS.

surface (Figure 7C). The enlarged image shows the algal surface covered by ACE2 receptors. Moreover, the unmodified algae incubated with fluorescent anti-ACE2 antibodies, compared to bare algae, exhibited a negligible alteration in GFP fluorescence intensity. However, they showed a significant increase, reflecting the effective combination of ACE2 receptors onto algae through click chemistry. The pseudo-colored SEM images of the ACE2-algae robot are further illustrated in

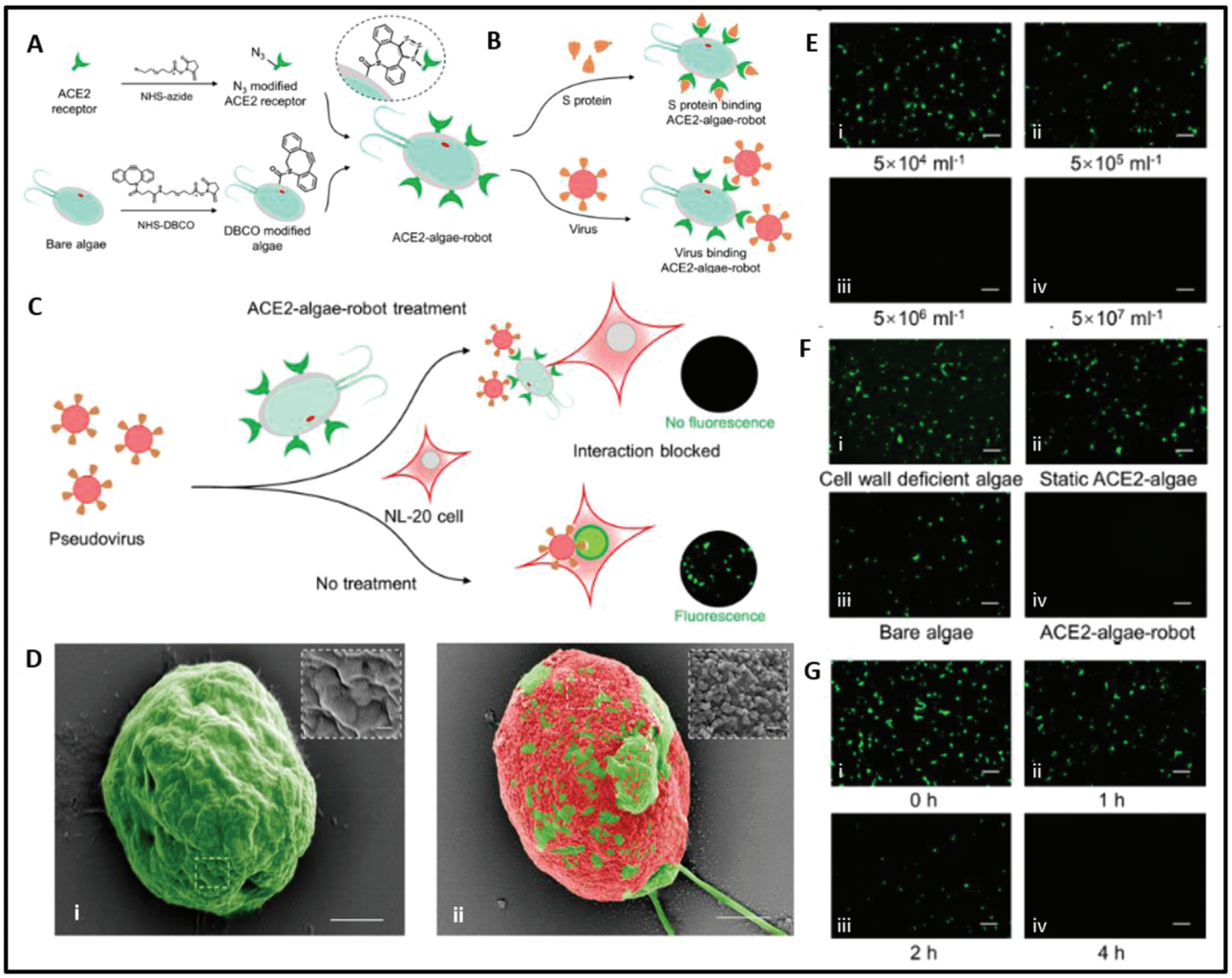

Figure 7. A) Illustration of the ACE2 receptor functionalized microalgae (ACE2-algae-robot). B) Illustration of the binding and removal of spike protein and SARS-CoV-2 virus on the ACE2-algae-robot. Zoom-in images show the surface morphology of the ACE2-algae-robot. C) Illustration of the viral removal by the ACE2-algae-robot by blocking the virus from penetrating into cells. D) i) before and ii) after contact with the virus. Scale bar: 200 nm. E) Fluorescent images of NL-20 cells infected with virus treated by different densities of the ACE2-algae-robot. Scale bar: 100 µm. F) Fluorescent images of NL-20 cells infected with the virus treated by the ACE2-algae-robot, bare algae, static ACE2-algae, and algae with cell wall deficiency. Scale bar: 100 µm. G) Fluorescent images of NL-20 cells infected with the virus are treated by the ACE2-algae-robot for different times (0, 1, 2, and 4 h). Scale bar: 100 µm. Reproduced with permission.[11] Copyright 2021, American Chemical Society.

Figure 7D; the attachment of virus particles can be seen on the ACE2-algae robot. Figure 7E,F shows the fluorescent images of NL-20 cells infected with the virus treated with different densities of the ACE2-algae robot, cells treated by the ACE2-algae robot, bare algae, static ACE2-algae, and cell wall-deficient algae and treated by the ACE2-algae robot for different periods.[11]

4. Micro–Nanosystems Properties

Humans, animals, and plants have different "operating systems," however they may have the same purpose or they may complement each other. Herein, we present the properties of micro–nanosystems from plants that can be used for fabrication with different applications.

4.1. Surface Roughness (Hydrophobicity and Hydrophilicity of Plants)

Compared to organisms such as humans and animals, plants show diversity in the structure and morphology of their leaf surfaces and provide multifunctional properties.[115] The hydrophobicity of the cuticle in the outer plant layer overcomes the physical and physiological problems related to an ambient environment, stabilizes the plant tissue, and has several protective properties concerning nastic and tropic movement.[14] Plant surfaces containing cuticles exhibit hydrophobicity because they mainly consist of a matrix of insoluble polyesters called cutin and soluble lipids called wax, which vary among plant species and organs.[116] Cuticles prevent the leaching of ions from inside the cells to the environment to reduce water loss. A broad spectrum of plant surface structures has a significant

influence on particle adhesion. These properties can contribute to the advancement of tissue engineering, particularly for structures that require hydrophobic and hydrophilic surfaces. As shown in **Figure 8**A, there are several essential functions of the plant boundary layer on a hydrophobic microstructured surface. These functions include i) a transport barrier to limit uncontrolled water loss and leaching from interior and foliar uptake; ii) surface wettability; iii) antiadhesive self-cleaning properties (lotus effect) to reduce contamination, pathogen attack, and attachment and locomotion of insects; iv) signaling to provide cues about host-pathogen and insect recognition, and epidermal cell development; v) changes in optical properties; vi) mechanical properties, which include resistance toward mechanical stress and maintenance of physiological integrity; and vii) increase turbulent air flow over the boundary air layer to reduce the surface temperature. These properties exhibit different phenotypic traits for each species. The visual appearances of macroscopic structures on some plant surfaces, as shown in Figure 8B, are because of the different properties of the microstructures. For example, *Magnolia grandiflora* has smooth and glossy surface textures owing to the thin layers of cuticles, as shown in Figure 8B-i. For *Dahlia sp*. in Figure 8B-ii, the surface appears velvety because of the convex microstructures of the epidermis cells. *Leucadendron argenteum* leaves have a silvery appearance, as shown in Figure 8B-iii, caused by a dense layer of light-reflecting hairs. In Figure 8B-iv, *Eucalyptus macrocarpa*

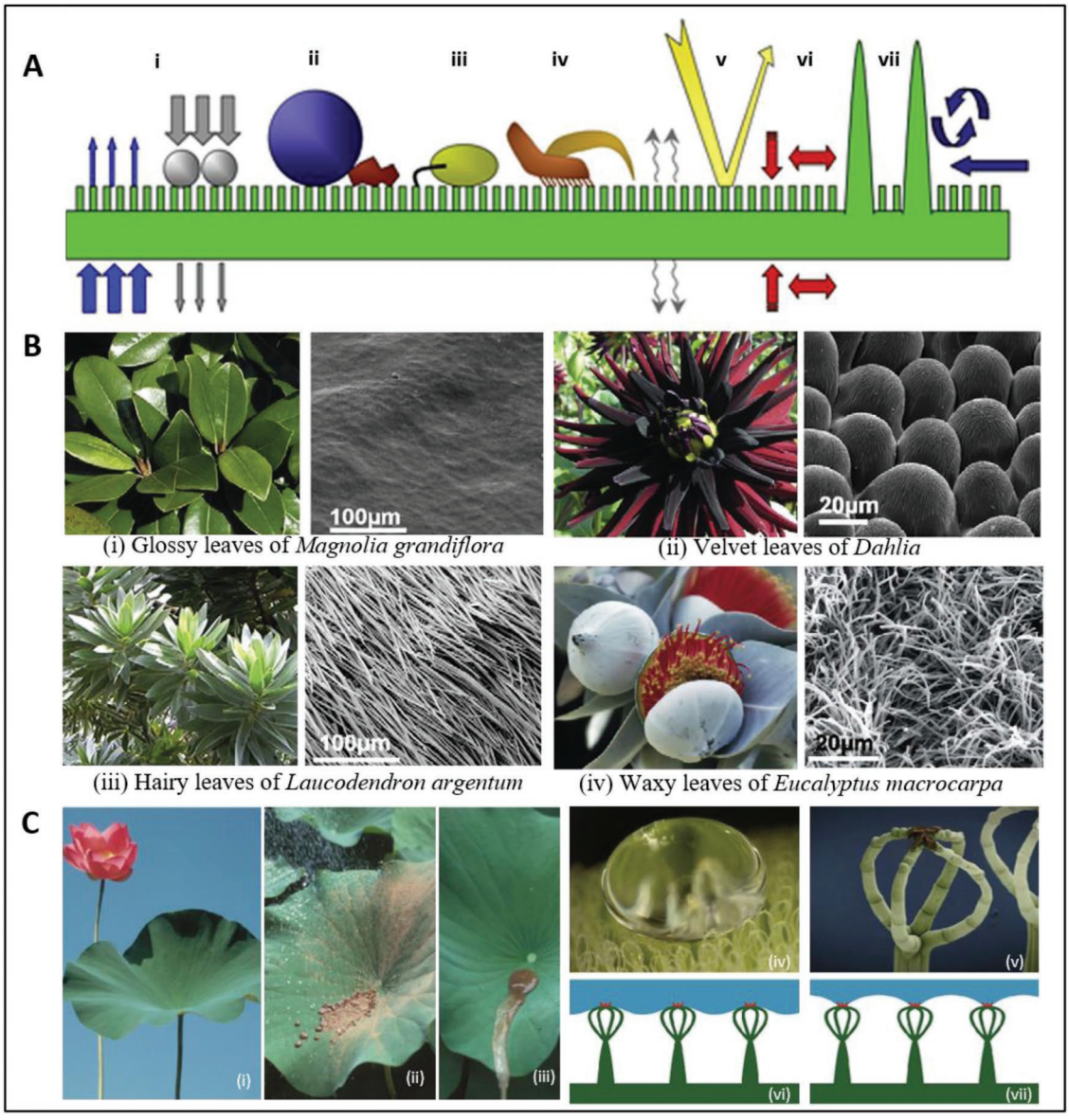

Figure 8. A) Hydrophobic ultrastructure depiction of the most important function of the boundary layer on the plant surface. B) The macroscopically visible plant surface optical appearance and their microstructures shown on the SEM micrographs. C) Superhydrophobic and the self-cleaning surface of i–iii) Lotus (*Nelumbo nucifera*) from dirt by water and iv–vii) superhydrophobic structure of *Salvinia* sp. leaf with egg batter-like surface and schematic illustration of the air–water interface on dynamically hydrostatic conditions. Reproduced under the terms of the CC-BY license.[14] Copyright 2017, Springer Nature.

leaves and flower bud surfaces appear white or bluish, which is caused by a dense covering of thread-like wax crystals.[14]

Evolutionary optimized wettable or nonwettable surfaces may be observed in water and wetland plants, including the water-repellent leaves of a lotus (*Nelumbo nucifera*). The cuticles impart hydrophilicity through supplying a complete wet surface or water spreading in submerged water-growing plants and a few tropical and subtropical plants, respectively, as in pitcher plants (*Nepenthes* sp.). Furthermore, the plant cuticle plays a vital role in interactions between insects and microorganisms. It protects plants against overheating by reflecting radiation and heat transfer via turbulent airflow and convection.[3]

Lotus leaf surfaces are made up of randomly distributed micro-papillae (diameter 5–9 mm) covered by fine branch-like nanostructures with a concurrence that confers high water contact and slight sliding angles. This multiscale surface and hydrophobic epicuticular wax induce superhydrophobic and low adhesion properties. This structure imparts a self-cleaning property called the lotus effect allowing spherical water droplets rolling on lotus leaves to easily pick up dirt particles and clean their surface.[117–119] Inspired by the lotus effect, several different composite approaches have been developed, including the construction of superhydrophobic self-cleaning surfaces with less water adherence by multiscale structural surface properties.[119–121] Considering this phenomenon, Lee et al. in 2009 fabricated a superhydrophobic coating using isotactic polypropylene (i-PP) surface gel-like porous structures with a water contact angle of 160°.[122] Duval and Gaboriaud in 2010 produced micro-to-nanoscale fibers or particles using the electrohydrodynamic (EHD) technique, a multipurpose and effective method.[123] Darmanin and Guittard in 2015 used the EHD method to prepare lotus-leaf-like microspheres and nanofibers with a superhydrophobic porous composite structure, which increased the surface roughness and contributed to the superhydrophobicity and 3D network to reinforce the composite film formed by interweaving nanofibers.[124]

The wettability, large surface area, flexibility, and superhydrophobic films of lotus leaves inspired Xu et al. to produce a thermal dispersion of silver nanoparticles to design a flexible hemisphere arrangement and modify it with 1-dodecanethiol.[125] The stratification of the acquired biomimetic film is identical to that of natural lotus leaves, consisting of hierarchical micro–nanostructures and large water contact and small sliding angles that provided remarkable superhydrophobicity and good flexibility for this type of biomimetic polymer film.[16] Some plant leaves exhibit superhydrophilicity if the contact angle with water is smaller than 108°, such as in pitcher plants. Plant surfaces can absorb water or spread it over their surfaces. Examples of leaves with water-absorbing porous surface structures are shown in Figure 8C. The structures of these plant surfaces can be used to develop adhesive or sticky characteristics.[3] Some plants, such as *Nephentes*, have slippery wax layers to capture and retain insects on their pitcher-like leaves to trap and digest insects.[126,127] A layer of 3D wax platelets caused a slippery zone in the pitcher-like tube above the digestive area in these species. Wax plays a critical role in prey trapping and retention[128] because they cannot attach to and walk on these waxy surfaces. The structure can develop surface characteristics with a self-cleaning ability and drag reduction.[3]

Several plants have hairs (also known as trichomes) on their surface. The hairs are found on most flowering plants, some conifers, and moss aerial surfaces.[129] The structures of these hairs are often complex and have different functions from one plant to another.[130] Some plants in dry habitats appear white because of their densely covered, air-filled hair that reflects visible light. They can affect water loss and surface wettability. However, it also acts as an anchor for seed dispersal. Some hairs form hook-like structures for climbing purposes, such as the kidney shoots (*Phaseolus vulgaris*) and *Cynoglossum officinale*.[129,130] These hook-like structures inspired the invention of Velcro in 1955. Velcro is derived from velour (velvet) and crochet (hook). It originated from the observation on the fruits of the burdock plant consisting of hooks, and their spines were tipped with tiny loops that stick out from the seeds and provide a hook-and-loop construction, which can grip or release instantly with minimal force. One side had stiff hooks as burs and the other had loops in the fabric.[3]

4.2. Nastic and Tropic Movements based on Osmotic Actuation

Plants provide an excellent source of inspiration for internal movements and are widely recognized as an example of low power consumption and energy efficiency. This concept originates from plant survival and adaptive growth in challenging dynamic environments, combined with a high actuation force and a rich movement repertoire. Plants tune their stiffness and achieve macroscopic movement to coordinate and perform reversible intracellular turgor modulation (pressure). Turgor, known as the uptake of water by cells, generates pressure created by water or solvent flux sustained by the osmotic pressure difference between the osmotic potentials inside and outside the cell. Water flux occurs through an osmotic membrane, so the plant adaptively responds to environmental stimuli.[131] Plants extensively employ osmotically generated pressure gradients for water and solution supporter and transporter,[132] and also to change turgor inside different cells in response to external stimuli has evolved in certain specialized plants. The opening and closing of guard cells in leaves or the swift nastic motions of *Mimosa pudica* in response to touch via clusters of motor cells called *pulvini*, making it sensitive to stimuli, are actuated by these turgor shifts. The use of osmotic gradients to accomplish mechanical work inspired by the plants, an osmosis-driven device with a high osmolarity could serve as a method to liberate potential energy from the chemical liquid through pressure generation, simply by watering the device. Furthermore, some studies on the dynamics of osmotically driven pressure generation have been conducted due to the potential usefulness of this information for actuating shape-changing materials.[133]

Plants utilize elastic energy to move swiftly, which is released by swelling and shrinking, resulting in a snap–buckling mechanism (observed in *Dionaea muscipula*). Lunni et al. in 2020 investigated hygroscopic bistable structures using electrospinning to develop a mechanism.[134] Plants are also a source of inspiration for the development of innovative biorobotic systems based on the synergistic integration of structural and multifunctional material properties, as demonstrated by Sinibaldi

and Mazzolai in 2020. They developed the dynamic behavior of two exemplary embodiments of an osmotic actuator model based on the osmotic principle in soft biorobotics.[131] The osmotic pressure gradient creates a critical driving force by separating compartments with different solute concentrations across a semipermeable membrane. If the one side volume expansion of the membrane is limited, the established concentration gradient will create a pressure gradient. Using an osmotically swollen hydrogel compartment in a micropump, Good et al. in 2007 examined and modeled liquid displacement.[135] In addition, the movement mechanism of carnivorous underwater traps (*Aldovandras vesiculosa*) is because of tissue's swelling and shrinking around the midrib, rather than mechanical buckling in *Dionaea muscipula*. Rapid plant movement results from tropical and nastic movements controlled by osmotic pressure, causing the tissues to swell and shrink based on the environment.[136] This factor shows that osmotic pressure is closely related to the bending–twisting and swelling–shrinking properties of plants.

4.3. Bending–Twisting and Swelling–Shrinking Properties

Plant tissues are composite materials consisting of hierarchical structures, many of which exhibit high stiffness, strength, and resilience like in woods. Some also show rapid fluid movements like in carnivorous plants. In a controlled manner on some plants, dead tissues can change shape according to external conditions, such as temperature or humidity.[137,138] Some plants like the Venus flytrap exhibit fast and fluid movements due to leaf lobes contracting during the closure. The entire leaf's shape changes from convex to concave, purposing a mechanically bistable structure with two stable states (open-close configurations and intermediate states). Controlled action by swelling and shrinking motor cells surrounding the midrib of an *Aldovandras vesiculosa* trap shows reversible movements when closing and opening the traps. Furthermore, rapid catapulting movements exhibited by Sundew (*Drosera glanduligera*) are caused by two possible mechanisms: 1) the hydraulic pressure change caused by rapid transport of water or 2) sudden loss of turgor pressure. However, this catapulting movement is irreversible. *Mimosa pudica* exhibits a fast, protective response to external stimuli, such as the leaves closing and pulvinus bending stimulated by a change in turgor pressure increasing the water potential in the extensor cells and water loss in flexor cells, hence the leaflet then folds up and ensnaring the trapped prey.[136] These examples show that changes in osmotic pressure can affect certain plants' bending–twisting and swelling–shrinking movements.

The distinction in shape actuates movement of dispersion and mobility of seed that is assisted by wheat awns attached to the seed. The cellulose fibrils on a single awn are parallel and randomly oriented to each other. This is causing differential swelling on awn's side, resulting in a reversible bending by the change in humidity. Repeated differences in humidity from the day/night temperature changes push the seed into the soil.[137] The tension of wood fibers at the upper parts of hardwoods branches is another example of shape change.[138] Sidorenko et al. in 2007 developed a hydrogel matrix embedded with stiff parallel silicon needles to set the movement in composite mimicking plant cells.[139] The presence of undeformable elements hinder the isotropic swelling of the matrix and the gel resulting in anisotropic deformation.[3]

4.4. Energy Conversion and Harvesting by Chloroplast

The detection of electrical potential within plants while decreasing carbon dioxide (CO_2) and keeping the surrounding temperature makes plants a valuable alternative energy source considering the energy crisis and environmental concerns. The fundamental properties of trees as renewable energy sources have become a critical study area.[140] Chloroplasts trap the sunlight radiation energy and conserve some of it in a stable chemical form. The energy produced by light-dependent reactions is subsequently used to reduce inorganic carbon dioxide to organic carbon in the sugar form.[141]

Several energy conversing and harvesting techniques have been adapted for plants. First, using electrostatic, piezoelectric, and electromagnetic transducers, the energy from any mechanical movement, such as motion and vibration, emits kinetic energy and can be converted into electrical energy.[142–144] An example of a piezoelectric transducer (PZT) is to cause twisting in any movement or tremors[145] on the piezoelectric capacitor to generate voltages. The higher the vibration frequency, the higher the amount of energy generated. The harvesting efficiency can be improved by matching the appropriate battery structure[146] and material[147] of the PZT. This device is known as a micromachine (≈1–10 mm) that produces low power. Electrical polarization behaviors are produced by any deformation or bending of PZT crystals, which can be expressed by mechanical and electrical equations.[140] Energy harvesting is one of the most exciting applications of piezoelectric materials, for both bulk materials and nanostructures. Wearable or implantable energy-harvesting devices development can generate electrical power produced by the vibrations related to biofluid fluxes or body movement, which are vital to empower biomedical devices. An example is the piezoelectric application of zinc oxide (ZnO) nanoparticles as biosensors because ZnO nanoparticles are widely known for their antibacterial activity.[141]

Second, the energy from sunlight can generate electricity by jumping electrons over the material and moving them via a wire. Instead, plant cells absorb light energy and displace it chemically into a protein. There is an energy source called a photon that can carry electromagnetic forces. Free electrons and holes are formed when atoms in the cathode (N-type silicon) absorb photons of light by releasing electrons; thus, it provides sufficient energy to jump out of the reduction zone. Electrons flowed through the wire, connecting the cathode to the anode (p-type silicon). There are four steps in the process of converting light into electric current in organic solar cells that became an inspiration to develop photovoltaic cells: i) forming an excited state or electron–hole pair (exciton) by absorbing photons; ii) diffusion of the exciton in a region, where iii) the separation of charge is occurring; and iv) supplying a direct current to the consumer loads, the charge is transported to the anode (holes) and cathode (electrons).[148] Solar energy indirectly has vast potential for harvesting energy from trees that

grow in the direction of sunlight. If this photovoltaic system is installed on a plant, the collection rates of sun irradiance can be obtained more frequently because most plants always point to the sun, and thus a solar tracker will no longer be needed. Solar cells with built-in harvesting leaves have been successfully applied in indoor environments.[149]

Finally, the energy from the electrode potential, which acts as a terminal completing the circuit, plays a vital role in the plant energy harvesting system. Oxidation and reduction of the electrode, built with the correct materials and a suitable medium, can generate an appropriate amount of energy.[140] Living plants can also be used as renewable energy resources using specific techniques. The first technique is a plant-microbial fuel cell (P-MFC), a biological fuel cell with a bioelectrochemical system that transforms energy when microbes move from natural electron acceptors, e.g., oxygen and nitrate, to an insoluble acceptor MFC anode. The system included an anaerobic anode chamber and an aerobic cathode chamber. These two chambers are secluded by an anion exchange membrane or a proton exchange membrane. The oxidation of the substrate in the anode chamber is transferred to the cathode after the release of electrons through the outlying wire with a resistor containing a conductive material. Electrons move to the anode via direct electron transfer,[150] electron mediators, or shuttles.[151] The second technique is the living plant bio-energy fuel cell, which uses voltage differences to monitor plant activity. Tress have electrical properties,[152] making them an exciting energy harvesting source; the electrical properties are thought to be because of the "streaming potential" mechanism.[153] This is because of the pressure gradient (flow of liquid) through a charged capillary, membrane, plug, or diaphragm, which has a potential difference at zero current produced by the convective flow of charge.[154]

Over the few decades behind, significant attention is received by the photocatalysis and electrocatalysis, owing to the demand for sustainable medical technologies. The approaches of photo- and electrocatalysts rely on electronic excitation, and the performance rely on the ability to create electron (e^-) hole (h^+) pairs that consecutively lead the chemical reactions with other compounds via oxidative (e.g., $2H_2O(l)/O_2(g) + 4H^+ (aq) + 4e^-$) and reductive reactions (e.g., $2H^+ (aq) + 2e^-/H_2(g)$). Several advanced nanomaterial-based photo- and electrocatalysts have been synthesized and reported and provide large surface-to-volume effects, numerous catalytically active sites, quantum size effects, and high stability advantages. These are considered as promising for energy and environmental applications, including photo- and electro water splitting to produce hydrogen (H_2) and carbon dioxide (CO_2) conversion. Furthermore, they are used for water treatment and disinfection in the fuel industry, air purification, and self-cleaning surfaces.[155]

5. Fabrication and Application in Biomedical Engineering

5.1. 3D and 4D Bioprinting

De Focatiis and Guest in 2002 developed a simple model using tree leaves deployed with different assembly arrangements to produce polygonal foldable membranes for deployable structures. These novel fold patterns were presented in a preliminary study for biomimetic thin membrane structures to extend the folding of natural structures, such as leaves, into engineering architectures.[156] Inspired by *Dionaea muscipula* or Venus flytrap, Lee et al. in 2010 developed a swelling-induced snap-buckling jumping microgel device that can generate high-speed actuation and effectively incorporate the elastic stability of the stored energy produced to rapidly release it from the device. In this actuation, the device can jump by itself, and through capillary action, the solvent used fills all the microfluidic networks in the device. Even after the solvent encircle the legs evaporates, the embedded microfluidic channels are still filled with solvent, resulting in outward bending of the legs, making them ready to jump. Then, the snap-buckling motion through the de-swelling process brings the legs back to their original shape as the solvent further evaporates. The fast movement produces sufficient force to jump out of the initial field of view.[157]

Bassik et al. in 2010 reported hydrogel bilayers as hinges (**Figure 9**A), designed to resemble the structure of a Venus flytrap, to actuate integrated actuator structures, and a straightforward design entirely fabricated by polymers that are mostly composed of rigid polymeric SU-8 panels. The workflow starts from the lithographic fabrication of bilayer structures composed of poly (ethylene oxide) diacrylate/*N*-isopropylacrylamide-acrylic acid (PEODA/NIPAm-AAc) and was prepared by spin coating a PEODA solution (solution 1). Solution 2 (NIPAm-AAc) was then put on the top of solution 1. The polymerized patterns then washed by the ethanol and are developed. The hydrogel bilayer was placed in aqueous solution 1 under a specific pH and ionic strength (IS) until equilibrium was reached. It was then transferred into solution 2 with different pH IS values compared to solution 1. This treatment causes the NIPAm-AAc (gel 1) to swell in response to the solution changes, whereas PEODA (gel 2) is not swelling and causing the fold of the bilayer. Transferring the bilayer into solution 1 causes gel 1 to deswell, and the bilayer unfolds in response to environmental changes. Exposing the bilayer gel on the solution at pH 7.8 at an ion strength of 0.2 M will achieve reversible folding over several minutes. The original solution (pH 7.8; IS 0.2 M) was then introduced to reach maximum swelling and accordingly unfold the bilayer by repeating it over five cycles. The reversibility of folding for more than 15 cycles makes the bilayer gel a highly biocompatible, eco-friendly, polymeric, self-assembling instrument that has potential applications in medical and biological fields, particularly in 3D cell culture, drug delivery, and noninvasive microsurgery.[158] The biomedical applications of the plant-derived biomimetic biomaterials are summarized in **Table 3**.

Yoon et al. in 2014 developed similar structures, but pointed at functional applications, such as self-folding polymeric microcapsules, untethered microgrippers, and thermally steered micromirror systems.[159] Wei et al. in 2014 reported a novel strategy to achieve programmable shape-changing of hybrid hydrogel sheets by modulating the mechanical properties of the in-plane and out-of-plane mismatches. The results from both experiments and computational analysis show that the shape changes of hybrid hydrogel sheets exhibit rich properties (e.g., movement direction, axis, and chirality) and multipurpose

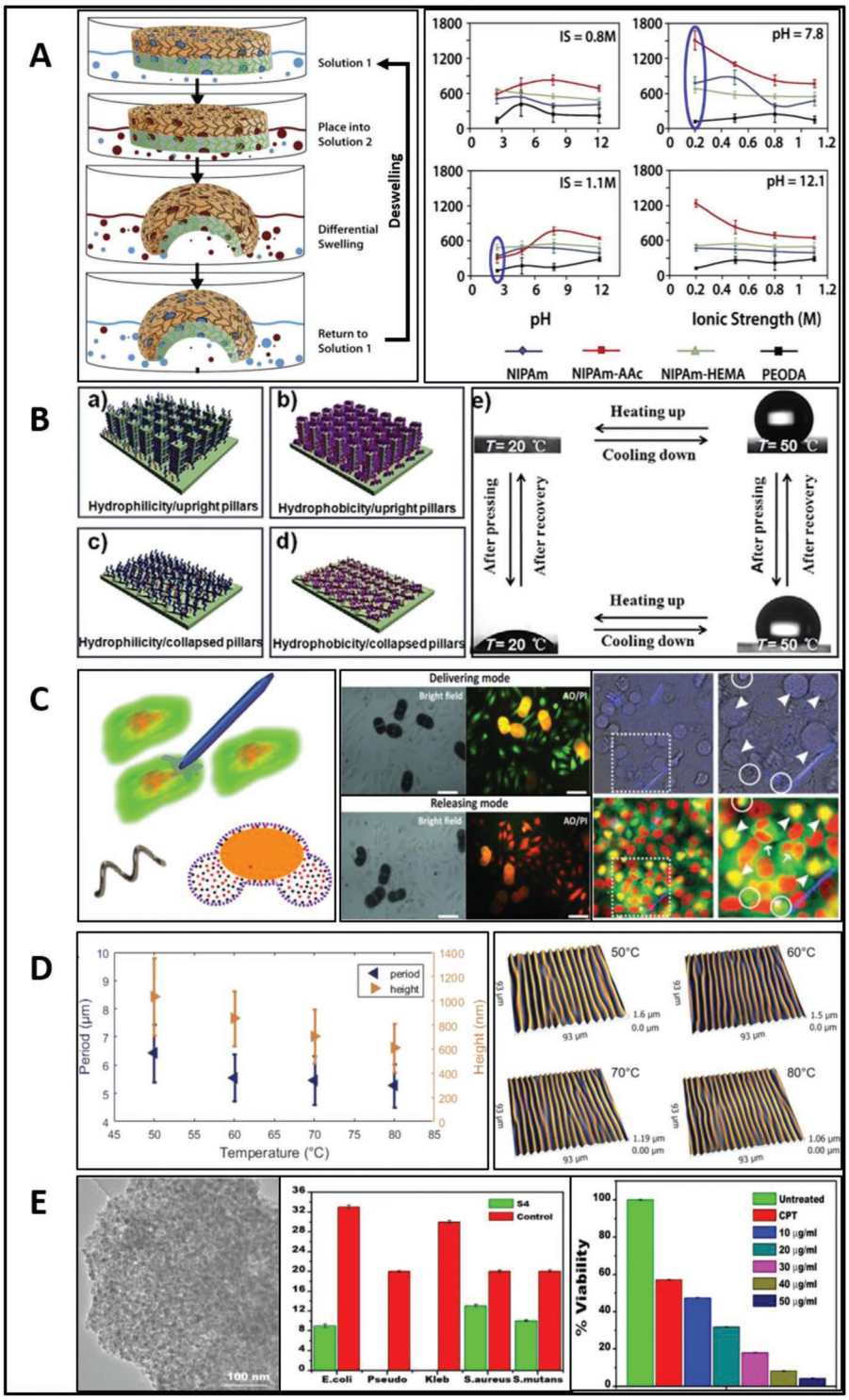

Figure 9. Biomedical application of plant-derived micro–nanoengineered biomaterial. A) Photopatterned actuators, composed of stimuli-responsive hydrogel bilayers made from *N*-isopropyl-acrylamide (NIPAm), acrylic acid (AAc), and poly-ethylene oxide diacrylate (PEODA) showed average swelling ratio of the hydrogel peaked at pH 7, 8 and IS 1,1 M. Reproduced with permission.[158] Copyright 2010, Elsevier. B) There are many kinds of micromotor for drug delivery. Green cells show that the pollen micromotor successfully delivered the drug and after releasing it, the cells are dead shown by the red color. Microdaggers also show anticancer activity after releasing anticancer drug successfully shown by the lysis of the cancer cells. Reproduced with permission.[105] Copyright 2016, Wiley. Reproduced with permission.[12] Copyright 2018, Wiley. C) a–d) The microstructures of the controlled surface wettability and (e) shows the shapes of water droplets correspond to the four states of microstructures. Reproduced with permission.[15] Copyright 2019, Wiley. D) Temperature-sensitive hierarchical micro–nanowrinkles SMP. Reproduced with permission.[180] Copyright 2017, RSC Publishing. E) *Withania somnifera–Eclipta prostrata*-doped TiO_2-NP exhibited good antibacterial activity against both gram-positive and gram-negative bacteria and as the concentration increases, cell viability decreases which in turn increases the anticancer activity. Reproduced with permission.[63] Copyright 2020, Wiley.

Table 3. Biomedical application of micro–nanoengineered biomaterials.

Name	In-plant principal	Application in biomedical	Work principal	Ref.
Hydrogel polymers for 4D bioprinting	Insect-trapping action of Venus flytrap	Jumping microgel device	Generates a snapping motion within 12 ms, The snap-buckling mechanism is responsible for the quick actuation	[157]
		Smart photopatterned bilayer hydrogel actuators	Photopatterned actuators, stimuli-responsive hydrogel bilayers (pH and ionic strength), actuate bilayer structures into 3D structures	[158,159]
		Braided hydrogel polymers	Using braided fibers hydrogel polymer, stiffness tunable actuators with and force generation capacity	[160]
Hydrogel composites	Shape-transforming leaf of Venus flytrap and awns of wild oats	Hybrid hydrogel	Dynamically transform into shapes such as helical sheets with reversible chirality	[161]
		Photo-origami designs	React to specific wavelengths of light, fold into exact 3D structures from 2D sheets like leaf folding patterns	[156,162]
Ionic polymer–metal composites (IPMCs)	Rapid muscular movements of Venus flytrap	A novel flytrap-inspired robot	Biomimetic sensor and actuator properties which characterize sensing and mechanical bending in an electrical field, resemble the Venus flytrap leave.	[163,164]
Osmotically actuated shape-changing structures	Hydraulic movements of Venus flytrap and sensitive plant	Reservoir chamber (RC)	Chamber filled with solution and the actuation of the chamber filled with solute and solvent is separated by a solute-impermeable osmotic membrane. The two models are different in their implementation of the actuator: 1. actuation work stored on the elastic deformation of a spring by a piston that displaces through solvent flux 2. actuation work stored through the elastic deformation of a nonpermeable bulging membrane	[165]
		Model for morphing structures driven by pressure-actuated cellular structures	ATP in nastic membranes activates proton pumps, moves selected ions into a cylindrical inclusion, electrochemical gradient activates co-transporters and exchangers	[136,166,167]
	Plant nastic movements	Protein-driven selective transport and highly targeted drug or vaccine delivery devices	Voltage-gated ion channels to control the activation. Dual activation chamber capable to induce simultaneous swelling and shrinking	[136,166]
Microswimmer	*Agapanthus africanus* xylem duct	Drug carrier (Drug delivery system)	Magnetically propelled helical microswimmers from spiral vessels (xylem) of plants followed by coating with a magnetic nickel layer	[110]
Microdaggers	*Dracaena marginata* calcified biotubes	Drug carrier (Drug delivery system)	Magnetically actuated calcified porous microneedles/ microdaggers from the *Dracaena marginata* plant possessed with drug carrier capability and coated with an iron magnetic layer to facilitate cellular drilling	[105]
Microbot	*Agaricus bisporus* porous fragments	Drug carrier and loader (Drug delivery system)	Magnetic nanoparticles (FeONPs) and anticancer Dox carrier and loader	[168]
Shape memory polymer	Plant surface	Micro–nanowrinkles	Film on which a metal thin was deposited before compression. The strain history of the SMP at the local scale can be remembered by the wrinkles and then reflected in the color change, with the help of the rigid metal thin film	[169–171]
Hydrophobic surface (special wettability)	Lotus	Biopolymer film	Electro-hydrodynamics (EHD) technique, a lotus-leaf-like microspheres and nanofibers, super-hydrophobic porous composite structure, increased surface roughness, 3D network formed by interweaving nanofibers.	[16]

adjustability through various external stimuli, material properties, and pattern geometry. This study provides guidance for designing more precise and complex shape transformations of soft materials.[161] These shape-changing hydrogels are promising because of their adjustable responsiveness to external stimuli, such as temperature, light, humidity, electric current, pH, and ionic strength disparity.[161] These hybrid hydrogels have several potential applications in soft robotics,[172] as self-healing materials,[173,174] drug delivery,[175] bioreactors,[176] actuators,[177] and 3D cell culture.[178] The biomedical applications of plant-inspired micro–nanoengineered biomaterials are summarized in Figure 9.

Plant-based natural polymers meet the requirements of novel biomaterials with desirable properties for various engineering processes that require minimal chemical processing for industrial applications. Plant scaffolds have a significant advantage: they are easy to make and manipulate, pliable, and easily cut, fashioned, rolled, or stacked to form a range of different sizes and shapes. They are also renewable, easy to mass produce, and cost-effective.[179]

5.2. Drug Delivery Systems

Noninvasive procedures from injecting encapsulated drugs into the human bloodstream, transporting it to the target, delivering, and releasing the drugs for the specific treatment have been proposed as a leading-procedures for cancer therapy. Anticancer drugs loaded into microcapsules under an in vitro setup could be transported through the environment resembling human blood with alkaline pH to suspend the drug and then deliver it to the cancerous cells, which have an acidic pH causing apoptosis of the cell, as shown in Figure 9B.[181] Gao et al. in 2014 reported a novel plant-derived approach to prepare high-yield, cost-effective magnetically propelled helical microswimmers directly from isolated spiral vessels (xylem) of plants, followed by magnetic nickel layer coating, as shown in **Figure 10**A. The plant material used in this system was derived from *Agapanthus africanus* xylem duct (Figure 10B), which lends to the biodegradability, biocompatibility, and ease of fabrication of the microswimmer; the magnetic layer allows precise control of the direction and high-speed corkscrew propulsion (Figure 10C–E). This method offers a simple and cost-effective fabrication route for the mass production of defined and effective helical magnetic swimmers compared to generic methods to fabricate actuated helical microswimmers magnetically by utilizing the intrinsic natural structures of plant xylem spiral vessels and controlling the geometric variables of the vessels, such as pitch and helix diameter. These plant-derived helical microswimmers show significant potential for future biomedical applications, such as advanced technology for noninvasive surgery, particularly because they can be propelled at high speeds in pure human serum.[110]

Bhuyan et al. in 2017 developed a simple, cost-effective, and magnetically controlled micromotor synthesized from mesoporous edible button mushrooms coated with magnetite nanoparticles. Micromotors mimicking microorganism movements exhibited a chemotactic response using external alkali and acid stimuli by migrating toward or away from the chemical trigger. Micromotors with a negative ζ-potential could be loaded with the cationic anticancer drug doxorubicin to perform drug release control toward the vicinity of HeLa cells under in vitro conditions. The efficiency of the micromotors compared to that of the simple drug was found to be significantly higher in inducing cell apoptosis. The report holds significant advantages in developing mushrooms as biocompatible and effective drug delivery vectors under pH-responsive systems through self-propelling micromotors, apart from being a rich dietary food source. Mushrooms can be considered a smart alternative for controlled drug delivery applications against synthetic materials with minimal side effects, which introduces new opportunities for mushroom-based prospective biomaterials for theranostic applications.[168]

Srivastava et al. in 2016 presented "dual-action microdaggers," the first proof-of-concept in which plant-derived biogenic micromotors from *Dracaena marginata* exhibit dual functionality: to create a cellular incision and facilitate highly localized drug administration through drug release, as shown in **Figure 11**. The drug release property can be used to kill the harmful malignant cells or release supplementary medicine for the cells for better competition against some infections. The loading of the anticancer drug camptothecin on calcified biotubes derived from idioblast cells is shown in Figure 11A and its structural properties are shown in Figure 11B. These biotubes allow site-specific activation of the drug in HeLa cancer cells in an acidic environment.[182,183] This study shows that the "dual-action" (i.e., cell-microdrilling and drug release) of biogenic hybrid micromotors potentially achieve single-cell target precision of noninvasive surgery together with the additional advantage of the drug release property to act as a package of "drug-rehabilitating cellular microsurgery." Calcified porous microneedles (40–60 μm long) extracted from *Dracaena marginata*[184,185] possess drug carrier capabilities (potentially calcium-based drug carriers),[186,187] and are coated with a magnetic layer to facilitate microdrilling by external magnetic actuation. It should be noted that such calcified biotubes are present in several plant species, scattered among both photosynthetic and nonphotosynthetic plant tissues under specialized cells termed idioblasts.[188] This development of the next-generation concept for "drug rehabilitation microsurgery" feature is first introduced, where cancerous or infected cells can be targeted by drug release of anticancer or supplementary medication. The ability of the microdagger to drill into a single cell can also be adopted as an anchoring mechanism for docking the subsequent release of other drug-mediated secondary treatments. This dual functionality of microdaggers will significantly reduce the treatment regimens associated with damage, such as chemotherapy. Finally, in the future, this type of micromotor will be influenced significantly by the choice of propulsion medium and technique, target-specific signaling sensors (microsensors) or real-time imaging modalities, and high-volume power equipped with a robust controlling system.[105]

Artificial micro–nanomotors with autonomous propulsion and capabilities to complete specific tasks have been developed as intelligent devices or platforms for biomedical applications. Various types of biocompatible and biodegradable materials, nature-derived polymers, and metals have been used for the construction of micro–nanomotors owing to their attractive physiological adaptive properties.[107] These biodegradable metals are metals and alloys that are expected to corrode gradually in vivo with an appropriate host response elicited by released corrosion products and then dissolve completely upon fulfilling the mission to assist with tissue healing with no implant residues.[189] Naturally available fuels, such as water, glucose, urea, and acid, are also utilized as substrates to improve their biocompatibility. Meanwhile, fuel-free micro–nanomotors with the input of external fields, such as magnetic, ultrasound, electric, and light fields, exhibit promising highly controllable properties and effective propulsion, eliminating the use of fuel. Moreover, to improve the biocompatibility of micro–nanomotors, it is important to formulate a feasible strategy for synthetic material combinations and biological components. Despite the immense progress that has been made to improve the systems, the application of these small-scale devices in real-world biomedicine is still in its infancy because the majority of micro–nanomotor frameworks that are currently available have problems with biodegradability. Considerable attention needs to be paid to improving the system and optimizing the current fabricated materials. Furthermore, one of the most effective ways to improve micro–nanomotors

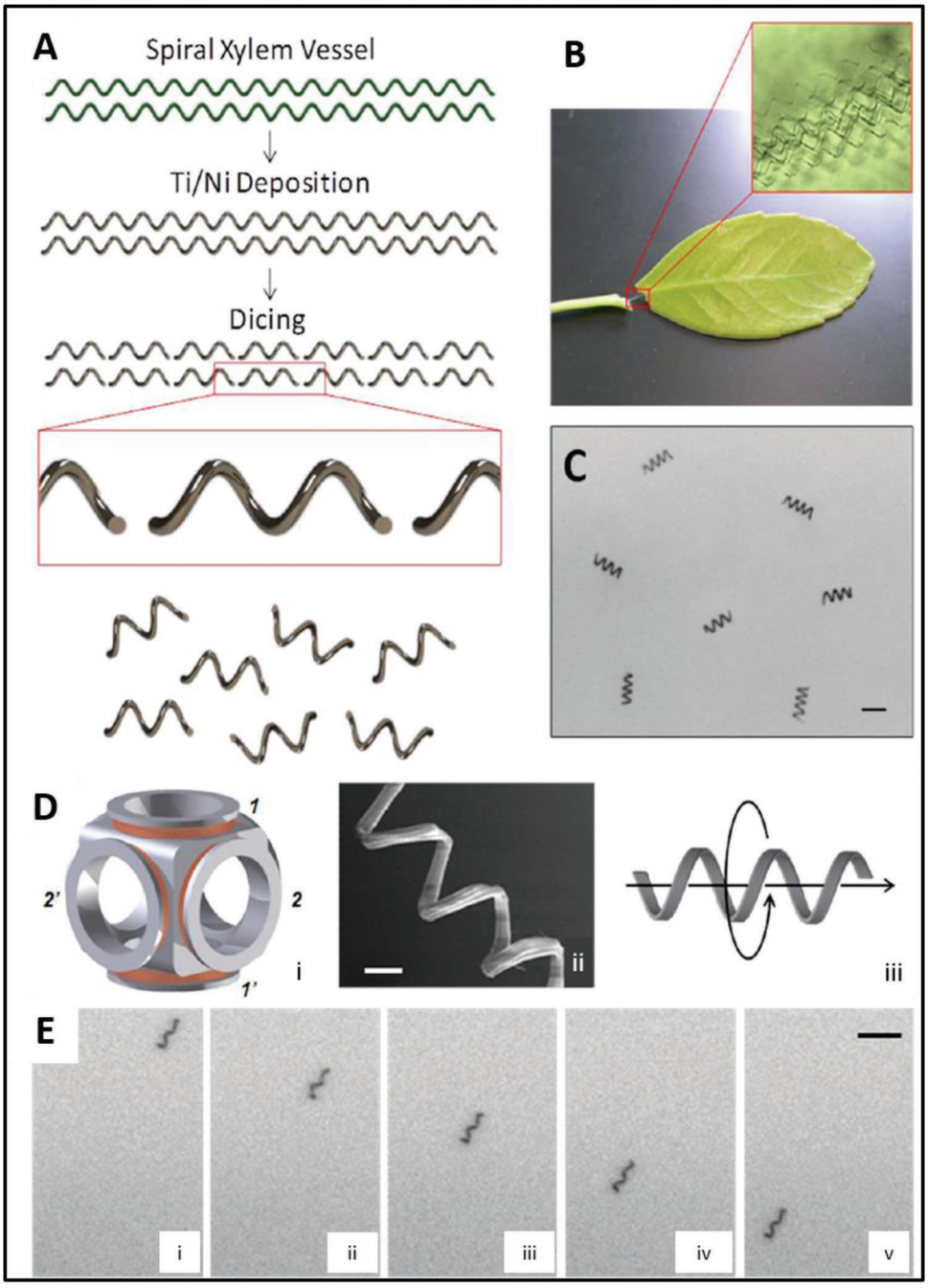

Figure 10. A) Plant-based microswimmers fabrication schematic. B) Optical microscopic image illustration of high density and uniformity of the natural helices. C) Microscope image of multiple magnetic helical microswimmers from *Agapanthus africanus*. Scale bar, 30 µm. D) i) The triaxial Helmholtz coil generates the rotating magnetic field. ii) SEM image of helical structure of a single microswimmer from *Raphiolepsis indica*. iii) Schematic of the corkscrew motion. Scale bar, 5 µm. E) i–v) Time lapse images depicting efficient propulsion of a helical microswimmer (from the spiral vessel of *R. indica*) under rotating magnetic field (10 G, 70 Hz) over 500 ms time intervals. Scale bar, 50 µm. Reproduced with permission.[110] Copyright 2014, American Chemical Society.

biodegradability is to use assembly materials such as supramolecular materials, layered nanomaterials, reversible bonded hydrogels, or physically responsive ingredients in construction. Another challenge faced by these systems is the identification of an appropriate energy source and propulsion mechanism to increase the in vivo biocompatibility. The low motion efficiency and short lifetime of fuel-powered micro–nanomotors are other concerns to be addressed because of the necessity to optimize the propulsion technique to achieve autonomous and effective propulsion without fuel systems. One promising approach to develop biocompatible micro–nanomotors is the development of biohybrid micromotor systems. Although further exploration

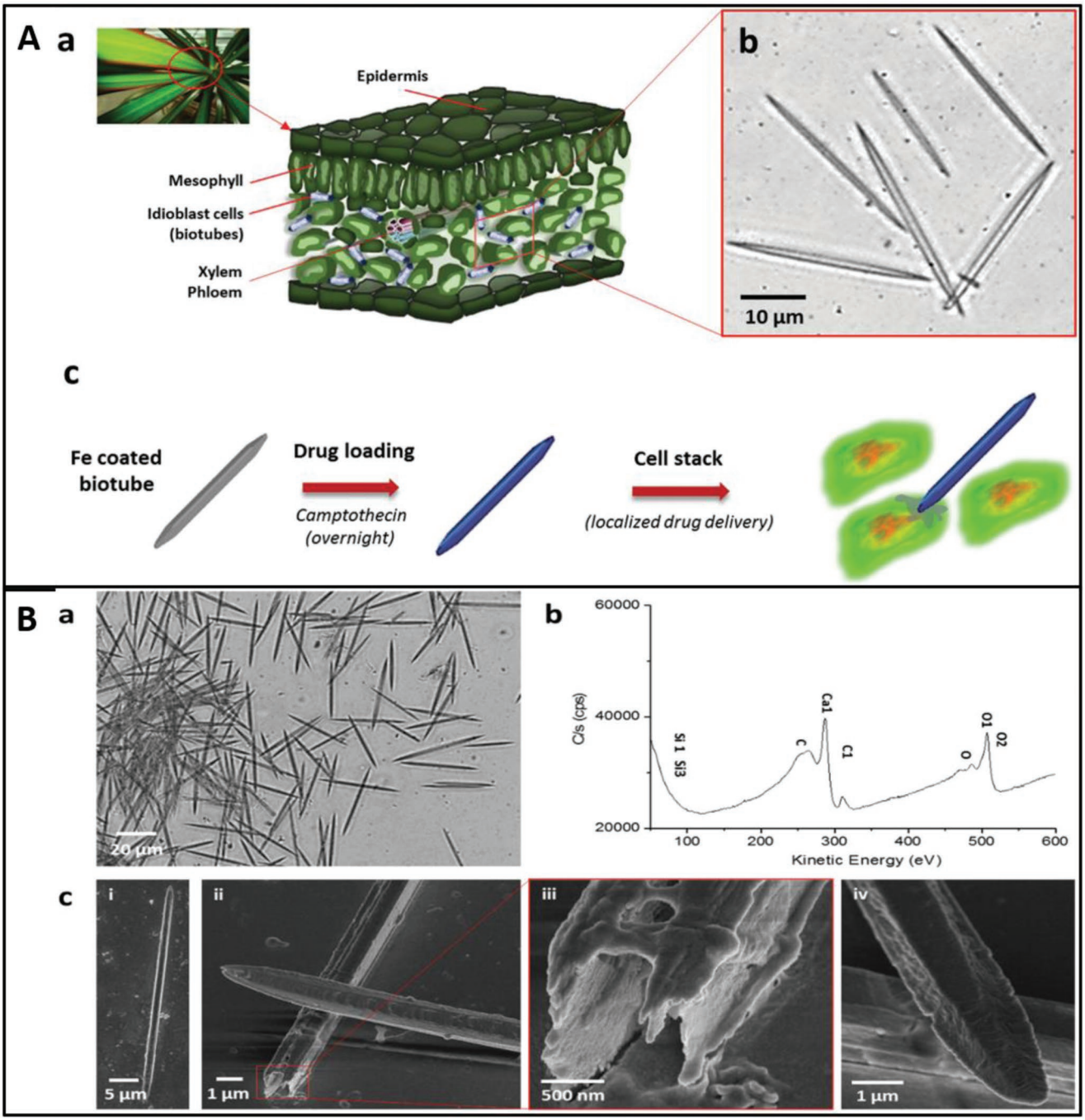

Figure 11. A) Schematics of biogenic microstructure extraction and the imparting of functional properties: a) *D. marginata* leaf highlighting plant cell walls. b) Calcified biotubes (raphides) present in the idioblast cells. c) Schematic representation of imparting magnetic and drug delivery properties to the biotube. B) Material characterization of biotubes: a) optical microscope image showing extracted calcified biotubes. b) XPS spectra of the unmodified biotube surface. c) SEM images showing i) single biotube, ii) surface of the biotubes with structural break, iii) inset highlighting internal cavity inside the porous biotube, and iv) edges running along the biotube. Reproduced with permission.[105] Copyright 2016, Wiley.

of the coupling method of artificial materials and biological components (e.g., living cells and bacteria) is required, there are disadvantages of biomimetic materials, such as poor flexibility, low structure controllability, and short service lifespan. Moreover, more attention should be paid to the components that could cause side effects, such as inflammatory responses or infections. The versatility of biomimetic system applications in the biomedical field, such as controlled drug release, multipurpose drug loading, precise imaging, and therapy must be explored further. Although the problems of this system have already been addressed, in vivo tests and safety assessments of micro–nanomotors applications require further exploration.[107]

Peng et al. in 2017 stated that micro–nanomotors at the cellular level could be applied as catalytic, fuel-free, and targeted

drug delivery motors and can accomplish locomotion inside and toward cells. Micro–nanomotor systems are a promising method in overcoming the cell barrier and direct the payload of drug delivery to target cells. Compared with passive drug-doped nanoparticles, active micro–nanomotors are superior in accessing solid tumor tissue cells, and high pressure blocks the entry of external molecules.[98]

5.3. Tissue Engineering

The electro-hydrodynamics (EHD) technique is a versatile and effective method for producing micro–nanofibers or particles.[119] Lotus-leaf-like microspheres and nanofibers with superhydrophobic porous composite structures were prepared using the EHD method.[125] The porous microsphere structure increases the surface roughness, which contributes to the superhydrophobicity and 3D network, which is formed by nanofiber interweaving to strengthen the composite film. The special wettability, large surface area, flexibility, and superhydrophobic film properties of lotus leaves also inspired the design of flexible hemisphere arrangements modified with 1-dodecanethiol using the fabricated thermal dispersion of silver nanoparticles.[123] The obtained biomimetic film stratification showed remarkable superhydrophobicity and good flexibility and was similar to the natural lotus leaves, which were built from hierarchical micro–nanostructure properties.[16] Figure 9C shows that the effect of controlled surface wettability can change the microstructures, and the shapes of water droplets can change corresponding to the four states of the microstructures.[15]

Advanced research has shown intelligent control of surface wettability by controlling the surface chemistry and microstructure. Surface chemistry is controlled by modifying the solid substrates of numerous responsive molecules (**Figure 12**A-a), which can easily transition between hydrophilicity and hydrophobicity to achieve a smart wetting performance. These properties have inspired the development of shape memory polymers (SMPs), which can recover their original shape after deformation under external stimuli (e.g., heat, light, and water).[190] SMPs have the ability to perform particular smart functions, such as switchable adhesion,[191] tunable optics,[192] and biomedical chips.[193] They also have unique advantages in that they can memorize and display various surface microstructure shapes, as displayed in Figure 12A-b, without external action assistance. However, contact angles and sliding angles (Figure 12C) of SMPs have several novel tunable functions (e.g., switchable isotropic and anisotropic wetting,[194] controllable gradient wetting,[195] and novel applications, such as rewritable platforms for droplet storage[196] and droplet transportation).[197] Moreover, combining responsive molecules and tunable SMP properties can achieve the coordinated regulation of surface chemistry and microstructure (Figure 12A-c). A schematic illustration of self-healing wetting on superhydrophobic SMP surfaces and wetting switching on superomniphobic SMP surfaces are shown in Figure 12D,E, respectively. Lotus-leaf-like hierarchical micro–nanostructures were prepared on a shape-memory epoxy resin substrate. They exhibited a crushed microstructure by pressing it and could be recovered by a heating process exhibiting self-healing ability (Figure 12D-a–f). The process of heating rearranges the surface chemical groups so that hydrophobic groups on polar and nonpolar groups exchange differentiation (Figure 12D-g–h). Similar to self-healing wetting, wetting switching on superomniphobic SMP surfaces can reversibly switch the shape between the original mushroom-like shape and collapsed shape by pressing it (Figure 12E-a–c). However, the superomniphobic surface water and oil (hexadecane) droplets have different switching properties, as water is always in the Cassie wetting state (Figure 12E-d–f). However, oil exhibited a highly adhesive Wenzel wetting state (Figure 12E-g–i). Finally, based on the excellent controlling ability of morphology and wettability of the SMP, the surface can be applied as a rewritable substrate to create different liquid patterns, as displayed by the patterns "UTD" and "CSU" shown in Figure 12E-j–k.[15]

5.4. Biosensing

Inspired by complex yet versatile leaf and petal surfaces, a mechanically directed self-assembly process with micro- and nanosized surface wrinkles, linearly oriented on an all-polymer bilayer system with a SMP substrate, was developed. The influence of the substrate programming strain and coating thickness on the wrinkle period and height was systematically investigated to determine a method to control the wrinkle size. The temperature during the recovery process can also be used to tailor the structural dimensions because the parameter is unique only to SMPs. Moreover, this method uses a biomimetic second structuring step of hierarchically structured petal surfaces of tulips and daisies to provide a large-scale, mold-free, and cost-effective way to fabricate a full polymer with adjustable structure size and intrinsic irregularity for self-cleaning surfaces and light management in solar cells in biomedical applications.[171,180]

Collaborative efforts in various fields, such as engineering, microbiology, physics, chemistry, biology, and biotechnology are required to develop biosensors owing to their versatility in different areas. The developed biosensors have been rigorously researched, including calorimetric and thermal detection, ion-sensitive, optical, piezoelectric, electrochemical, and immunobiosensors. For glucose sensing, two enzymes, namely, glucose oxidases (G-ox) and glucose dehydrogenases, are often used for large-scale glucose detection. Graphene-(G-ox) bio-composites displayed excellent sensitivity of 1.85 μA mM^{-1} cm^{-2} in a 0.1×10^{-3} to 27×10^{-3} M glucose range. The potential bio-application of the engineered biosensor over human serum was also studied, which exhibited precise sensitivity results when evaluating blood glucose levels.[16]

One of the main challenges of biosensing techniques is the time-consuming sample preparation. Fast or selective targeting and sensing of unprocessed biological samples using receptor-functionalized autonomously moving motors is a promising approach. The motion of micro–nanomotors provides a novel approach for detecting rRNA or other biomolecules.[198] This motor system has also been proven to successfully detect RNA not only secreted by cells but also inside the cells.[101] 1D plasmonic magnetic nanotubes incorporated with nickel nanomagnets and dual-surface-coated plasmonic silver nanoparticles have been reported to be used for sensing in

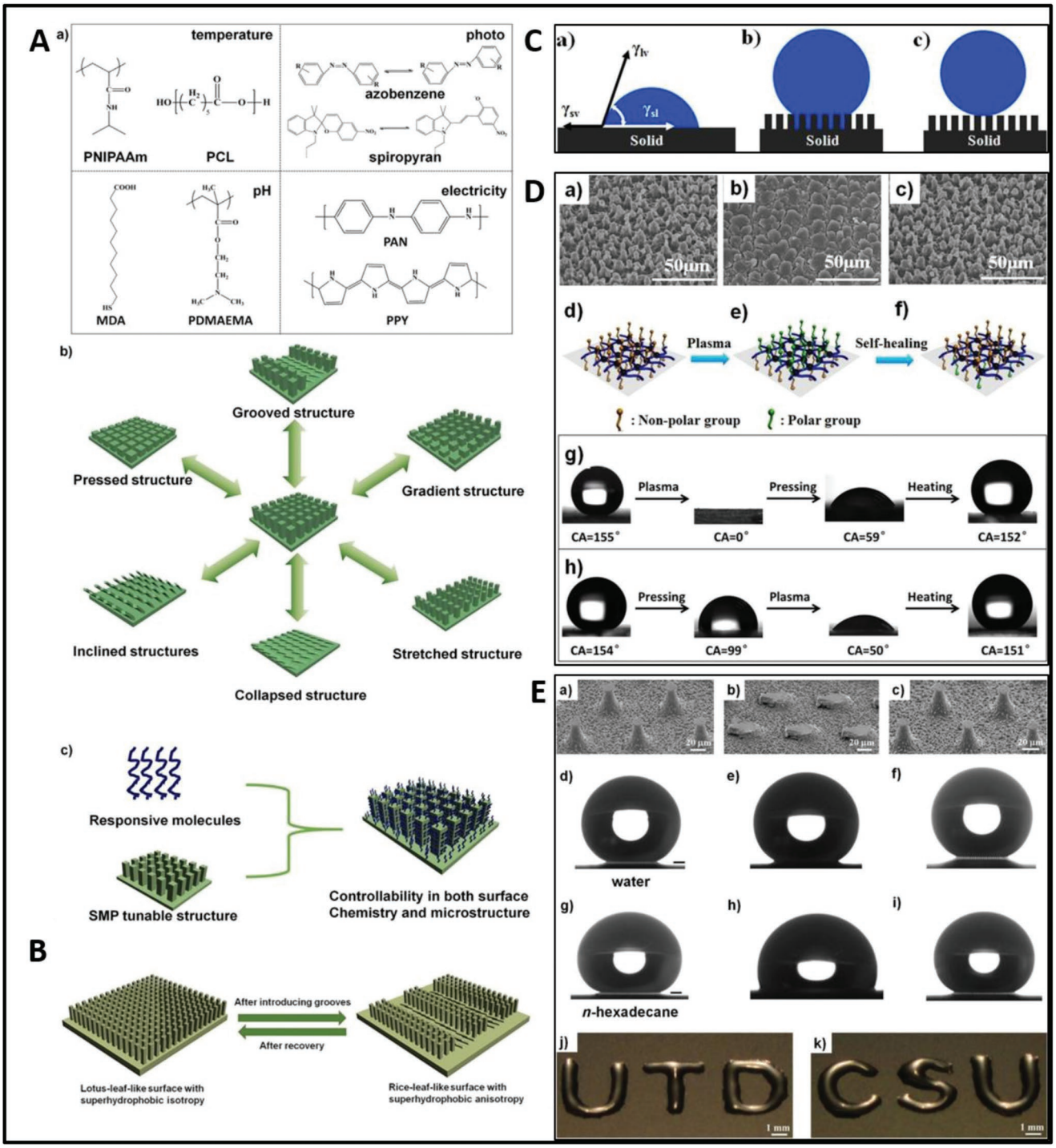

Figure 12. A) Strategy for smart wetting control inspired by Lotus leaf for shape changing polymer based on a) responsive molecules for surface chemistry control; b) SMPs for surface microstructure control; and c) coordinated regulation of both surface chemistry and microstructure. PNIPAAm = poly(*N*-isopropylacrylamide), PCL = polycaprolactone, MDA = 11-mercaptoundecanoic acid, PDMAEMA = poly(2-dimethylaminoethyl methacrylate), PAN = polyaniline, PPY = polypyridine. B) Schematic illustration of surface microstructure variation between two states. C) Schematic illustration of liquid/solid contact models: a) a flat surface, b) the Wenzel state, and c) the Cassie state. D) SEM images for SMP pillars in the a) original, b) deformed, and c) recovered shapes. d–f) Schematic illustration of surface group reorganization during plasma and heating processes. g,h) Shapes of a water droplet on the surface in different states. E) SEM images for SMP pillars in the a) original, b) collapsed, and c) restored shapes. d–f) Shapes of a water droplet on the surface corresponding to different pillar shapes. g–i) Shapes of a hexadecane droplet on the surface correspond to different pillar shapes. j,k) Different liquid patterns repeatedly created on the SMP surface. Reproduced with permission.[15] Copyright 2019, Wiley.

situ cell membrane composition.[199] The embedded nanomagnets and silver nanoparticles facilitated magnetic maneuvering and surface-enhanced Raman scattering detection. Typically, external chemical fuel utilization in the systems may interfere with detection results; therefore, motor systems that can utilize sample media or components are highly desirable. Future developments should consider the possible impact of any motor reaction or inducing pH changes on the sensing results.[98]

5.5. Antimicrobial, Anticancer, and Antioxidant

Micro–nanomotors doped with nanoparticles can act as delivery agents for therapeutic molecules and perform as therapeutic agents. An approach was developed to produce platinum nanoparticle-loaded polyelectrolyte microtube motors coated with gold nanoshells and tumor-targeting peptide T7 (containing the HAIYPRH sequence) on the surface. After localizing to the tumor cells, micromotors selectively recognize and target HeLa cells. No binding was observed between red blood cells (as control cells) and the tumor cells, but dissipated heat from the gold plasmon resonance upon using near-infrared, resulting in a temperature increase of ≈10 °C in the 70 mm range around the micromotors. Subsequent apoptosis of the targeted cells was observed, and in this case, the micromotors were demonstrated to be photothermal agents for the selective eradication of cancer cells.[98,102]

Plant-assisted synthesis of nanoparticles has important roles in biomedical applications, as shown in Table 1. Silver (Ag), gold (Au), platinum (Pt), and palladium (Pd) nanoparticles mostly have antimicrobial and anticancer properties.[34,43,57,61] Ag can also degrade hazardous chemical rye[32] and improve catalytic performance.[33] In addition to these roles, the bimetallic structure of silver–iron (Ag–Fe) nanoparticles contains antifungal agents derived from *Beta vulgaris*.[38] Copper (Cu) and bimetal gold–silver (Au–Ag) exhibit enhanced wound-healing efficacy.[45,51] Cu, Pd, and Pt nanoparticles and selenium oxide (SnO_2) also exhibit antioxidant activity.[50,56,61,65] Pd, CuO, and SnO_2 exhibited the photocatalytic performance of nanoparticles.[53,58,65] *Withania somnifera-Eclipta prostrata*-doped TiO_2 nanoparticles shown in Figure 9E exhibited good antibacterial activity against both gram-positive and gram-negative bacteria, and as the concentration increased, cell viability decreased, which in turn increased the anticancer activity.[63]

Core–shell nanoparticles from plants have proven to be superior compared to bacteria and fungi in assisted processes. Plants are considered suitable candidates for large-scale expeditious green synthesis of nanoparticles and a higher rate of synthesis compared to processes aided by microorganisms. Moreover, the nature of extract has a notable effect on the availability of functional groups, such as aldehydes, carboxyls, hydroxyls, and aminos on nanoparticle surfaces, which can bind to a variety of biological structures, including DNAs, proteins, antibodies, polymers, and enzymes. These choices of extracts have advantages such as reduction of the metals salts.[200] Therefore, determining the interaction of nanoparticles from plants is necessary to understand the synthesis from different aspects and to have better strategies for addressing challenges and future prospects of their use in therapeutic and pharmacological applications for various diseases and types of cancer.[201]

6. Conclusions and Future Perspectives

We reported some recent studies on plant-actuated micro–nanorobot platforms, including their structural design, functionality prospects, and promising applications in the biomedical field. Through a strategic implementation of the bottom-up and top-down approaches of biomimetics, plant systems that only work on the plant itself can be utilized and adapted into new emerging technologies in robotics. Current studies indicate that plant-derived micro–nanomaterials have several benefits for biomedical applications, such as being highly biocompatible, efficient, cost-effective, and safe, which contributes to a sustainable world. There are several sources of micro–nanostructures of plants, such as nanoparticles derived from plant extracts, which can be a valuable resource for various biomedical applications (e.g., 3D bioprinting, enhanced tissue engineering, drug delivery systems, biosensors, and antimicrobial and anticancer applications). Furthermore, the development of micro–nanostructures on broader integrated systems, such as nanofiber composites and nanoporous materials, provides a promising and important role in several fields, including 3D and 4D bioprinting, drug delivery systems, and surface wettability. Moreover, naturally modified micro–nanomotors are expected to meet the challenges of biocompatibility and targeted delivery in cancer therapy. Plant micro–nanosystems also enable it to adapt to new novel technologies in micro–nanoscale biomedical fields. For example, the surface wettability of plants plays an important role in maintaining dual surface switchable wettability based on the environment. The energy conversion and harvesting properties of chloroplasts can be used to create a piezoelectric device that can be used to conduct green energy. Osmotic actuation also plays an important role in rapid nastic movements to provide no-muscle movements and activate bending–twisting and swelling–shrinking properties, which then become an inspiration for soft robotics and SMPs.

However, some points need to be addressed for further improvement. Biomimetics provide a platform to mimic the structure of nature and adapt it to other synthetic structures. However, it is challenging to directly emulate the functionality perfected over centuries of evolution into a novel structure. The motions of micro–nanomotors with micro- and nanoscale entities propelled in solution are governed by diverse and contradictory behaviors of physical laws when compared to macroscale systems. Smaller matter in large volumes has a larger exposed area than a large object, which is susceptible to a high rate of energy dissipation compared to its ability to store the required fuel. Therefore, external sources of power that harness the systems are preferred to propel motors.

In addition, the prominent viscous drag relative to the fluids becomes particularly challenging to move on small-scale motors. Consequently, a low-Reynolds number system governs the motion, which is significantly different from the macroscale matter. Therefore, it is mandatory to detect a clear displacement

of the movement by disturbing the symmetry of the systems through a suitable design of the motor, geometry, and surface chemistry.

The applicability of micro–nanomotors for in vivo applications is also challenging. The immune system of the body is the largest barrier to in vivo applications because it is recognized as a foreign material. Therefore, the motor systems need to conquer it with a high level of precision to target a specific site, particularly to reach remote locations by penetrating several layers of tissues and cells.

Developing micro–nanomotors into readily available and mass-produced materials still needs to pass commercially realistic parameters (e.g., ease of fabrication, mass producibility, and cost-effectiveness). Therefore, it is essential to match the design, composition, and propulsion mechanisms to these aspects. Novel plant-actuated micro–nanomaterials have different structures compared to materials that are mass produced nowadays and are still superior in terms of practicality and durability. In addition, continuous efforts and hard work are required to improve the quality of plant-derived products so that mass-production can be achieved.

Therefore, scientists continue to pursue the first step toward a green and sustainable planet and develop plant-based nanomaterials as an emerging material source with a wide range of applications, particularly in fast-paced biomedical engineering. Moreover, the future of nanomedicine will depend on the rational engineering of various nanomaterials with controlled physicochemical properties to dictate their interactions in an anticipated manner with biological systems for biomedical applications. Additionally, a detailed and thorough understanding of nano-bio interactions from several sources, such as the plant systems mentioned in this paper, is required to discover favorable physicochemical characteristics of various nanomaterials, which may render them more responsive toward the inner biological environment for therapeutic benefits without any toxic impacts.

Acknowledgements

R.L. and T.V.P. contributed equally to this work. The Basic Science Research Program supported this work through the National Research Foundation of Korea (NRF) funded by the Ministry of Education (nos. 2018R1A6A1A03025582, 2019R1D1A3A03103828, and 2022R1I1A3063302), Republic of Korea.

Conflict of Interest

The authors declare no conflict of interest.

Keywords

biomedical applications, biomimetics, micro–nanomotors, micro–nanorobots, plant actuated

Received: March 7, 2022
Revised: June 14, 2022
Published online:

[1] S. Srivastava, P. Goyal, in *Novel Biomaterials* (Eds: R. Allan, U. Förstner, W. Salomons), Springer Berlin Heidelberg, Berlin, Heidelberg **2010**, pp. 93–96.
[2] G. K. Gupta, S. De, A. Franco, A. Balu, R. Luque, *Molecules* **2015**, *21*, 48.
[3] B. Bhushan, *Philos. Trans. R. Soc., A* **2009**, *367*, 1445.
[4] A. Barhoum, J. Jeevanandam, A. Rastogi, P. Samyn, Y. Boluk, A. Dufresne, M. K. Danquah, M. Bechelany, *Nanoscale* **2020**, *12*, 22845.
[5] H. Chandra, P. Kumari, E. Bontempi, S. Yadav, *Biocatal. Agric. Biotechnol.* **2020**, *24*, 101518.
[6] K. Moraczewski, T. Karasiewicz, B. Jagodziński, A. Trafarski, A. Pawłowska, M. Stepczyńska, P. Rytlewski, *Sustainable Mater. Technol.* **2021**, *30*, e00351.
[7] B. Mazzolai, C. Laschi, P. Dario, S. Mugnai, S. Mancuso, *Plant Signaling Behav.* **2010**, *5*, 90.
[8] G. Wan, C. Jin, I. Trase, S. Zhao, Z. Chen, *Sensors* **2018**, *18*, 2973.
[9] T. M. Allen, P. R. Cullis, *Science* **2004**, *303*, 1818.
[10] Y. Zhang, L. Zhang, L. Yang, C. I. Vong, K. F. Chan, W. K. K. Wu, T. N. Y. Kwong, N. W. S. Lo, M. Ip, S. H. Wong, J. J. Y. Sung, P. W. Y. Chiu, L. Zhang, *Sci. Adv.* **2019**, *5*, eaau9650.
[11] F. Zhang, Z. Li, L. Yin, Q. Zhang, N. Askarinam, R. Mundaca-Uribe, F. Tehrani, E. Karshalev, W. Gao, L. Zhang, J. Wang, *J. Am. Chem. Soc.* **2021**, *143*, 12194.
[12] M. Sun, X. Fan, X. Meng, J. Song, W. Chen, L. Sun, H. Xie, *Nanoscale* **2019**, *11*, 18382.
[13] S. Yu, Y. Zhang, H. Duan, Y. Liu, X. Quan, P. Tao, W. Shang, J. Wu, C. Song, T. Deng, *Sci. Rep.* **2015**, *5*, 13600.
[14] W. Barthlott, M. Mail, B. Bhushan, K. Koch, *Nano-Micro Lett.* **2017**, *9*, 23.
[15] D. Zhang, Z. Cheng, Y. Liu, *Chem. – Eur. J.* **2019**, *25*, 3979.
[16] T. R. Prianka, N. Subhan, H. M. Reza, M. d. K. Hosain, M. d. A. Rahman, H. Lee, S. Md. Sharker, *Mater. Sci. Eng., C* **2018**, *93*, 1104.
[17] O. Speck, T. Speck, *Biomimetics* **2021**, *6*, 49.
[18] T. Speck, O. Speck, in *Design and Nature IV* (Ed: C. A. Brebbia), WIT Press, Algarve, Portugal **2008**, pp. 3–11.
[19] D. Nath, P. Banerjee, *Environ. Toxicol. Pharmacol.* **2013**, *36*, 997.
[20] M. Razavi, E. Salahinejad, M. Fahmy, M. Yazdimamaghani, D. Vashaee, L. Tayebi, in *Green Processes for Nanotechnology* (Eds: V. A. Basiuk, E. V. Basiuk), Springer International Publishing, Cham **2015**, pp. 207–235.
[21] R. Mohammadinejad, A. Shavandi, D. S. Raie, J. Sangeetha, M. Soleimani, S. Shokrian Hajibehzad, D. Thangadurai, R. Hospet, J. O. Popoola, A. Arzani, M. A. Gómez-Lim, S. Iravani, R. S. Varma, *Green Chem.* **2019**, *21*, 1845.
[22] K. B. Narayanan, N. Sakthivel, *Adv. Colloid Interface Sci.* **2011**, *169*, 59.
[23] D. Hebbalalu, J. Lalley, M. N. Nadagouda, R. S. Varma, *ACS Sustainable Chem. Eng.* **2013**, *1*, 703.
[24] M. N. Nadagouda, G. Hoag, J. Collins, R. S. Varma, *Cryst. Growth Des.* **2009**, *9*, 4979.
[25] S. Jadoun, R. Arif, N. K. Jangid, R. K. Meena, *Environ. Chem. Lett.* **2021**, *19*, 355.
[26] G. A. Naikoo, M. Mustaqeem, I. U. Hassan, T. Awan, F. Arshad, H. Salim, A. Qurashi, *J. Saudi Chem. Soc.* **2021**, *25*, 101304.
[27] Y. Wang, D. O'Connor, Z. Shen, I. M. C. Lo, D. C. W. Tsang, S. Pehkonen, S. Pu, D. Hou, *J. Cleaner Prod.* **2019**, *226*, 540.
[28] N. A. I. Md Ishak, S. K. Kamarudin, S. N. Timmiati, *Mater. Res. Express* **2019**, *6*, 112004.
[29] M. Nadeem, D. Tungmunnithum, C. Hano, B. H. Abbasi, S. S. Hashmi, W. Ahmad, A. Zahir, *Green Chem. Lett. Rev.* **2018**, *11*, 492.
[30] J. Iqbal, B. A. Abbasi, T. Mahmood, S. Kanwal, R. Ahmad, M. Ashraf, *J. Mol. Struct.* **2019**, *1189*, 315.

[31] T. U. Doan Thi, T. T. Nguyen, Y. D. Thi, K. H. Ta Thi, B. T. Phan, K. N. Pham, *RSC Adv.* **2020**, *10*, 23899.
[32] V. K. M. Katta, R. S. Dubey, *Mater. Today: Proc.* **2021**, *45*, 794.
[33] K. K. Bharadwaj, B. Rabha, S. Pati, B. K. Choudhury, T. Sarkar, S. K. Gogoi, N. Kakati, D. Baishya, Z. A. Kari, H. A. Edinur, *Nanomaterials* **2021**, *11*, 1999.
[34] V. Morales-Lozoya, H. Espinoza-Gómez, L. Z. Flores-López, E. L. Sotelo-Barrera, A. Núñez-Rivera, R. D. Cadena-Nava, G. Alonso-Nuñez, I. A. Rivero, *Appl. Surf. Sci.* **2021**, *537*, 147855.
[35] M. S. Jabir, Y. M. Saleh, G. M. Sulaiman, N. Y. Yaseen, U. I. Sahib, Y. H. Dewir, M. S. Alwahibi, D. A. Soliman, *Nanomaterials* **2021**, *11*, 384.
[36] S. N. Nangare, S. Landge, A. G. Patil, R. S. Tade, P. K. Deshmukh, P. O. Patil, *Adv. Nat. Sci.: Nanosci. Nanotechnol.* **2021**, *12*, 035004.
[37] M. A. Malik, A. A. Alshehri, R. Patel, *J. Mater. Res. Technol.* **2021**, *12*, 455.
[38] M. R. Kamli, V. Srivastava, N. H. Hajrah, J. S. M. Sabir, A. Ali, M. A. Malik, A. Ahmad, *Antioxidants* **2021**, *10*, 182.
[39] A. L. Padilla-Cruz, J. A. Garza-Cervantes, X. G. Vasto-Anzaldo, G. García-Rivas, A. León-Buitimea, J. R. Morones-Ramírez, *Sci. Rep.* **2021**, *11*, 5351.
[40] S. Jeyarani, N. M. Vinita, P. Puja, S. Senthamilselvi, U. Devan, A. J. Velangani, M. Biruntha, A. Pugazhendhi, P. Kumar, *J. Photochem. Photobiol., B* **2020**, *202*, 111715.
[41] M. M. Zangeneh, A. Zangeneh, *Appl. Organomet. Chem.* **2020**, *34*, e5271.
[42] P. Kharey, S. B. Dutta, A. Gorey, M. Manikandan, A. Kumari, S. Vasudevan, I. A. Palani, S. K. Majumder, S. Gupta, *ChemistrySelect* **2020**, *5*, 7901.
[43] P. Boomi, G. P. Poorani, S. Selvam, S. Palanisamy, S. Jegatheeswaran, K. Anand, C. Balakumar, K. Premkumar, H. G. Prabu, *Appl. Organomet. Chem.* **2020**, *34*, e5574.
[44] N. Ahmad, A. K. Sharma, S. Sharma, I. Khan, D. K. Sharma, A. Shamsi, T. R. Santhosh Kumar, M. Seervi, *Drug Chem. Toxicol.* **2019**, *42*, 43.
[45] M. Sharma, S. Yadav, N. Ganesh, M. M. Srivastava, S. Srivastava, *Prog. Biomater.* **2019**, *8*, 51.
[46] K. K. Masibi, O. E. Fayemi, A. S. Adekunle, E. M. Sherif, E. E. Ebenso, *Electroanalysis* **2020**, *32*, 2745.
[47] J. M. A. Villalobos-Noriega, E. R. Leon, C. Rodríguez-Beas, E. Larios-Rodríguez, M. Plascencia-Jatomea, A. Martínez-Higuera, H. Acuña-Campa, R. A. Iñiguez-Palomares, *Core-Shell Au@Ag Nanoparticles Synthesized with Polyphenols As Antimicrobial Agents*, **2021**, *16*, 118.
[48] E. Benassai, M. Del Bubba, C. Ancillotti, I. Colzi, C. Gonnelli, N. Calisi, M. C. Salvatici, E. Casalone, S. Ristori, *Mater. Sci. Eng., C* **2021**, *119*, 111453.
[49] M. W. Amer, A. M. Awwad, *Chem. Int.* **2021**, *7*, 1.
[50] S. Rajeshkumar, S. Menon, S. V. Kumar, M. M. Tambuwala, H. A. Bakshi, M. Mehta, S. Satija, G. Gupta, D. K. Chellappan, L. Thangavelu, K. Dua, *J. Photochem. Photobiol., B* **2019**, *197*, 111531.
[51] H. Zhao, H. Su, A. Ahmeda, Y. Sun, Z. Li, M. M. Zangeneh, M. Nowrozi, A. Zangeneh, R. Moradi, *Appl. Organomet. Chem.* **2020**, *34*, e5587.
[52] K. Velsankar, R. M. Aswin Kumar, R. Preethi, V. Muthulakshmi, S. Sudhahar, *J. Environ. Chem. Eng.* **2020**, *8*, 104123.
[53] S. Kayalvizhi, A. Sengottaiyan, T. Selvankumar, B. Senthilkumar, C. Sudhakar, K. Selvam, *Optik* **2020**, *202*, 163507.
[54] A. Dey, S. Manna, S. Chattopadhyay, D. Mondal, D. Chattopadhyay, A. Raj, S. Das, B. G. Bag, S. Roy, *J. Saudi Chem. Soc.* **2019**, *23*, 222.
[55] R. Chandrasekaran, S. A. Yadav, S. Sivaperumal, *J. Cluster Sci.* **2020**, *31*, 221.
[56] S. A. Fahmy, I. M. Fawzy, B. M. Saleh, M. Y. Issa, U. Bakowsky, H. M. E.-S. Azzazy, *Nanomaterials* **2021**, *11*, 965.
[57] S. Gnanasekar, J. Murugaraj, B. Dhivyabharathi, V. Krishnamoorthy, P. K. Jha, P. Seetharaman, R. Vilwanathan, S. Sivaperumal, *J. Appl. Biomed.* **2018**, *16*, 59.
[58] C. Vijilvani, M. R. Bindhu, F. C. Frincy, M. S. AlSalhi, S. Sabitha, K. Saravanakumar, S. Devanesan, M. Umadevi, M. J. Aljaafreh, M. Atif, *J. Photochem. Photobiol., B* **2020**, *202*, 111713.
[59] A. Attar, M. Altikatoglu Yapaoz, *Prep. Biochem. Biotechnol.* **2018**, *48*, 629.
[60] R. Dobrucka, A. Romaniuk-Drapała, M. Kaczmarek, *Biomed. Microdevices* **2019**, *21*, 75.
[61] A. M. Selvi, S. Palanisamy, S. Jeyanthi, M. Vinosha, S. Mohandoss, M. Tabarsa, S. You, E. Kannapiran, N. M. Prabhu, *Process Biochem.* **2020**, *98*, 21.
[62] N. S. Al-Radadi, S. I. Y. Adam, *Arabian J. Chem.* **2020**, *13*, 4386.
[63] P. Maheswari, S. Harish, M. Navaneethan, C. Muthamizhchelvan, S. Ponnusamy, Y. Hayakawa, *Mater. Sci. Eng., C* **2020**, *108*, 110457.
[64] S. Majeed, M. Danish, M. H. B. Ismail, M. T. Ansari, M. N. M. Ibrahim, *Sustainable Chem. Pharm.* **2019**, *14*, 100179.
[65] S. Begum, M.d. Ahmaruzzaman, *J. Photochem. Photobiol., B* **2018**, *184*, 44.
[66] B. Joseph, V. K. Sagarika, C. Sabu, N. Kalarikkal, S. Thomas, *J. Bioresour. Bioprod.* **2020**, *5*, 223.
[67] T. V. Patil, D. K. Patel, S. D. Dutta, K. Ganguly, T. S. Santra, K.-T. Lim, *Bioact. Mater.* **2022**, *9*, 566.
[68] H. M. C. Azeredo, M. F. Rosa, L. H. C. Mattoso, *Ind. Crops Prod.* **2017**, *97*, 664.
[69] O. Nechyporchuk, M. N. Belgacem, J. Bras, *Ind. Crops Prod.* **2016**, *93*, 2.
[70] X. Yang, M. S. Reid, P. Olsén, L. A. Berglund, *ACS Nano* **2020**, *14*, 724.
[71] F. Azzam, L. Heux, J.-L. Putaux, B. Jean, *Biomacromolecules* **2010**, *11*, 3652.
[72] D. Klemm, F. Kramer, S. Moritz, T. Lindström, M. Ankerfors, D. Gray, A. Dorris, *Angew. Chem., Int. Ed.* **2011**, *50*, 5438.
[73] L. K. Kian, M. Jawaid, H. Ariffin, Z. Karim, *Int. J. Biol. Macromol.* **2018**, *114*, 54.
[74] M. Ramesh, K. Palanikumar, K. H. Reddy, *Renewable Sustainable Energy Rev.* **2017**, *79*, 558.
[75] Q. Zhao, H. J. Qi, T. Xie, *Prog. Polym. Sci.* **2015**, *49–50*, 79.
[76] M. Behl, A. Lendlein, *Mater. Today* **2007**, *10*, 20.
[77] M.d. W. Rahman, N. R. Shefa, *Adv. Polym. Technol.* **2021**, *2021*, 7848088.
[78] D. Wang, M. D. Green, K. Chen, C. Daengngam, Y. Kotsuchibashi, *Int. J. Polym. Sci.* **2016**, *2016*, 6480259.
[79] D. Le Corre, J. Bras, A. Dufresne, *Biomacromolecules* **2010**, *11*, 1139.
[80] A. Dufresne, J.-Y. Cavaillé, W. Helbert, *Macromolecules* **1996**, *29*, 7624.
[81] J.-L. Putaux, S. Molina-Boisseau, T. Momaur, A. Dufresne, *Biomacromolecules* **2003**, *4*, 1198.
[82] Y. Chen, C. Liu, P. R. Chang, D. P. Anderson, M. A. Huneault, *Polym. Eng. Sci.* **2009**, *49*, 369.
[83] Y. Chen, X. Cao, P. R. Chang, M. A. Huneault, *Carbohydr. Polym.* **2008**, *73*, 8.
[84] H. Zheng, F. Ai, P. R. Chang, J. Huang, A. Dufresne, *Polym. Compos.* **2009**, *30*, 474.
[85] N. L. García, L. Ribba, A. Dufresne, M. I. Aranguren, S. Goyanes, *Macromol. Mater. Eng.* **2009**, *294*, 169.
[86] H. Namazi, A. Dadkhah, *J. Appl. Polym. Sci.* **2008**, *110*, 2405.
[87] H. Angellier, L. Choisnard, S. Molina-Boisseau, P. Ozil, A. Dufresne, *Biomacromolecules* **2004**, *5*, 1545.
[88] F. Fathi, A. Dadkhah, H. Namazi, *Int. J. Nanopart.* **2014**, *7*, 37.
[89] Y. Wang, L. Zhang, *J. Nanosci. Nanotechnol.* **2008**, *8*, 5831.
[90] Y. Xu, E. N. Sismour, C. Grizzard, M. Thomas, D. Pestov, Z. Huba, T. Wang, H. L. Bhardwaj, *Cereal Chem. J.* **2014**, *91*, 383.
[91] F. Jiang, Y.-L. Hsieh, *Carbohydr. Polym.* **2013**, *95*, 32.

[92] M. Kaushik, K. Basu, C. Benoit, C. M. Cirtiu, H. Vali, A. Moores, *J. Am. Chem. Soc.* **2015**, *137*, 6124.
[93] R. Mohammadinejad, S. Karimi, S. Iravani, R. S. Varma, *Green Chem.* **2016**, *18*, 20.
[94] P. Chen, L.-K. Wang, G. Wang, M.-R. Gao, J. Ge, W.-J. Yuan, Y.-H. Shen, A.-J. Xie, S.-H. Yu, *Energy Environ. Sci.* **2014**, *7*, 4095.
[95] H. Yang, X. Sun, H. Zhu, Y. Yu, Q. Zhu, Z. Fu, S. Ta, L. Wang, H. Zhu, Q. Zhang, *Ceram. Int.* **2020**, *46*, 5811.
[96] F. Si, Y. Zhang, L. Yan, J. Zhu, M. Xiao, C. Liu, W. Xing, J. Zhang, in *Rotating Electrode Methods and Oxygen Reduction Electrocatalysts* (Eds: W. Xing, G. Yin, J. Zhang), Elsevier, New York **2014**, pp. 133–170.
[97] M. Koleoso, X. Feng, Y. Xue, Q. Li, T. Munshi, X. Chen, *Mater. Today Bio* **2020**, *8*, 100085.
[98] F. Peng, Y. Tu, D. A. Wilson, *Chem. Soc. Rev.* **2017**, *46*, 5289.
[99] Z. Wu, Y. Wu, W. He, X. Lin, J. Sun, Q. He, *Angew. Chem., Int. Ed.* **2013**, *52*, 7000.
[100] M. Xuan, J. Shao, X. Lin, L. Dai, Q. He, *ChemPhysChem* **2014**, *15*, 2255.
[101] B. Esteban-Fernández de Ávila, A. Martín, F. Soto, M. A. Lopez-Ramirez, S. Campuzano, G. M. Vásquez-Machado, W. Gao, L. Zhang, J. Wang, *ACS Nano* **2015**, *9*, 6756.
[102] Z. Wu, X. Lin, Y. Wu, T. Si, J. Sun, Q. He, *ACS Nano* **2014**, *8*, 6097.
[103] E. S. Olson, J. Orozco, Z. Wu, C. D. Malone, B. Yi, W. Gao, M. Eghtedari, J. Wang, R. F. Mattrey, *Biomaterials* **2013**, *34*, 8918.
[104] V. Magdanz, M. Guix, F. Hebenstreit, O. G. Schmidt, *Adv. Mater.* **2016**, *28*, 4084.
[105] S. K. Srivastava, M. Medina-Sánchez, B. Koch, O. G. Schmidt, *Adv. Mater.* **2016**, *28*, 832.
[106] S. Sanchez, A. A. Solovev, Y. Mei, O. G. Schmidt, *J. Am. Chem. Soc.* **2010**, *132*, 13144.
[107] J. Ou, K. Liu, J. Jiang, D. A. Wilson, L. Liu, F. Wang, S. Wang, Y. Tu, F. Peng, *Small* **2020**, *16*, 1906184.
[108] L. Schwarz, M. Medina-Sánchez, O. G. Schmidt, *Appl. Phys. Rev.* **2017**, *4*, 031301.
[109] S. Iravani, R. S. Varma, *Nano-Micro Lett.* **2021**, *13*, 128.
[110] W. Gao, X. Feng, A. Pei, C. R. Kane, R. Tam, C. Hennessy, J. Wang, *Nano Lett.* **2014**, *14*, 305.
[111] T. Ariizumi, K. Toriyama, *Annu. Rev. Plant Biol.* **2011**, *62*, 437.
[112] R. C. Mundargi, M. G. Potroz, S. Park, H. Shirahama, J. H. Lee, J. Seo, N.-J. Cho, *Small* **2016**, *12*, 1167.
[113] M. G. Potroz, R. C. Mundargi, J. J. Gillissen, E.-L. Tan, S. Meker, J. H. Park, H. Jung, S. Park, D. Cho, S.-I. Bang, N.-J. Cho, *Adv. Funct. Mater.* **2017**, *27*, 1770184.
[114] G. Randrianarison, M. A. Ashraf, *Geol., Ecol. Landscapes* **2017**, *1*, 104.
[115] K. Koch, I. C. Blecher, G. König, S. Kehraus, W. Barthlott, *Funct. Plant Biol.* **2009**, *36*, 339.
[116] C. Ziv, Z. Zhao, Y. G. Gao, Y. Xia, *Front. Plant Sci.* **2018**, *9*, 1088.
[117] B. Aryal, G. Neuner, *Oecologia* **2010**, *162*, 1.
[118] B. Bhushan, in *Nanotribology Nanomechanics I* (Ed: B. Bhushan), Springer Berlin Heidelberg, Berlin, Heidelberg **2011**, pp. 1–34.
[119] Z. Guo, W. Liu, B.-L. Su, *J. Colloid Interface Sci.* **2011**, *353*, 335.
[120] K. Liu, Z. Li, W. Wang, L. Jiang, *Appl. Phys. Lett.* **2011**, *99*, 261905.
[121] T. Verho, J. T. Korhonen, L. Sainiemi, V. Jokinen, C. Bower, K. Franze, S. Franssila, P. Andrew, O. Ikkala, R. H. A. Ras, *Proc. Natl. Acad. Sci. USA* **2012**, *109*, 10210.
[122] S. Lee, J. H. Kang, S. J. Lee, W. Hwang, *Lab Chip* **2009**, *9*, 2234.
[123] J. F. L. Duval, F. Gaboriaud, *Curr. Opin. Colloid Interface Sci.* **2010**, *15*, 184.
[124] T. Darmanin, F. Guittard, *Mater. Today* **2015**, *18*, 273.
[125] M. Xu, N. Lu, H. Xu, D. Qi, Y. Wang, S. Shi, L. Chi, *Soft Matter* **2010**, *6*, 1438.
[126] B. E. Juniper, R. J. Robins, D. M. Joel, *The Carnivorous Plants*, Academic Press, London; San Diego, CA **1989**.
[127] K. Koch, B. Bhushan, W. Barthlott, in *Springer Handbook of Nanotechnology* (Ed: B. Bhushan), Springer Berlin Heidelberg, Berlin, Heidelberg **2010**, pp. 1399–1436.
[128] E. Gorb, K. Haas, A. Henrich, S. Enders, N. Barbakadze, S. Gorb, *J. Exp. Biol.* **2005**, *208*, 4651.
[129] K. Koch, B. Bhushan, W. Barthlott, *Prog. Mater. Sci.* **2009**, *54*, 137.
[130] G. J. Wagner, E. Wang, R. W. Shepherd, *Ann. Bot.* **2004**, *93*, 3.
[131] E. Sinibaldi, B. Mazzolai, in *2020 I-RIM Conf.* (Eds: B. Allotta, M. C. Carrozza, E. Menegatti, G. Oriolo), Zenodo, Geneva **2020**, p. 163.
[132] A. D. Stroock, V. V. Pagay, M. A. Zwieniecki, N. M. Holbrook, *Annu. Rev. Fluid Mech.* **2014**, *46*, 615.
[133] B. R. Bruhn, T. B. H. Schroeder, S. Li, Y. N. Billeh, K. W. Wang, M. Mayer, *PLoS One* **2014**, *9*, e91350.
[134] D. Lunni, M. Cianchetti, C. Filippeschi, E. Sinibaldi, B. Mazzolai, *Adv. Mater. Interfaces* **2020**, *7*, 1901310.
[135] B. T. Good, C. N. Bowman, R. H. Davis, *J. Colloid Interface Sci.* **2007**, *305*, 239.
[136] Q. Guo, E. Dai, X. Han, S. Xie, E. Chao, Z. Chen, *J. R. Soc., Interface* **2015**, *12*, 20150598.
[137] R. Elbaum, S. Gorb, P. Fratzl, *J. Struct. Biol.* **2008**, *164*, 101.
[138] P. Fratzl, R. Elbaum, I. Burgert, *Faraday Discuss.* **2008**, *139*, 275.
[139] A. Sidorenko, T. Krupenkin, A. Taylor, P. Fratzl, J. Aizenberg, *Science* **2007**, *315*, 487.
[140] T. H. Cheng, K. Bc, C. Uttraphan, H. Yee, *Int. J. Renewable Energy Res.* **2018**, *8*, 2398.
[141] *Piezoelectric Nanomaterials for Biomedical Applications* (Eds: G. Ciofani, A. Menciassi), Springer Berlin Heidelberg, Berlin, Heidelberg **2012**.
[142] S. Akkaya Oy, A. E. Ozdemir, in *2016 IEEE Int. Conf. Renewable Energy Research and Applications (ICRERA)* (Eds: I. Colak, F. Kurokawa), IEEE, Piscataway, NJ **2016**, pp. 63–66.
[143] A. E. Ozdemir, S. Akkaya Oy, in *2016 IEEE Int. Conf. Renewable Energy Research and Applications (ICRERA)* (Eds: I. Colak, F. Kurokawa), IEEE, Piscataway, NJ **2016**, pp. 59–62.
[144] R. J. M. Vullers, R. van Schaijk, I. Doms, C. Van Hoof, R. Mertens, *Solid-State Electron.* **2009**, *53*, 684.
[145] A. Raghavan, C. E. S. Cesnik, *Smart Mater. Struct.* **2005**, *14*, 1448.
[146] J. P. Ayers, D. W. Greve, I. J. Oppenheim, *Proc. SPIE 5057, Smart Structures and Materials 2003: Smart Systems and Nondestructive Evaluation for Civil Infrastructures* (Ed: S.-C. Liu), SPIE, San Diego, CA **2003**, p. 364.
[147] Z. L. Wang, J. Song, *Science* **2006**, *312*, 242.
[148] H. Hoppe, N. S. Sariciftci, *J. Mater. Res.* **2004**, *19*, 1924.
[149] L. Yerva, B. Campbell, A. Bansal, T. Schmid, P. Dutta, in *Proc. 11th Int. Conf. Information Processing in Sensor Networks – IPSN 12*, (Eds: A. Terzis, K. Whitehouse), ACM Press, New York, NY **2012**, pp. 197–208.
[150] D. R. Bond, D. R. Lovley, *Appl. Environ. Microbiol.* **2003**, *69*, 1548.
[151] K. Rabaey, N. Boon, S. D. Siciliano, M. Verhaege, W. Verstraete, *Appl. Environ. Microbiol.* **2004**, *70*, 5373.
[152] A. G. Volkov, J. Reedus, C. M. Mitchell, C. Tucket, V. Forde-Tuckett, M. I. Volkova, V. S. Markin, L. Chua, *Plant Signaling Behav.* **2014**, *9*, e29056.
[153] A. Labady, D. Thomas, T. Shvetsova, A. G. Volkov, *Bioelectrochemistry* **2002**, *57*, 47.
[154] D. L. Oatley-Radcliffe, N. Aljohani, P. M. Williams, N. Hilal, in *Membrane Characterization* (Eds: N. Hilal, A. F. Ismail, T. Matsuura, D. L. Oatley-Radcliffe), Elsevier, New York **2017**, pp. 405–422.
[155] T. Kawawaki, Y. Negishi, H. Kawasaki, *Nanoscale Adv.* **2020**, *2*, 17.
[156] D. S. A. De Focatiis, S. D. Guest, *Philos. Trans. R. Soc. London, Ser. A* **2002**, *360*, 227.
[157] H. Lee, C. Xia, N. X. Fang, *Soft Matter* **2010**, *6*, 4342.
[158] N. Bassik, B. T. Abebe, K. E. Laflin, D. H. Gracias, *Polymer* **2010**, *51*, 6093.

[159] C. Yoon, R. Xiao, J. Park, J. Cha, T. D. Nguyen, D. H. Gracias, *Smart Mater. Struct.* **2014**, *23*, 094008.
[160] C. Santulli, S. I. Patel, G. Jeronimidis, F. J. Davis, G. R. Mitchell, *Smart Mater. Struct.* **2005**, *14*, 434.
[161] Z. Wei, Z. Jia, J. Athas, C. Wang, S. R. Raghavan, T. Li, Z. Nie, *Soft Matter* **2014**, *10*, 8157.
[162] J. Ryu, M. D'Amato, X. Cui, K. N. Long, H. Jerry Qi, M. L. Dunn, *Appl. Phys. Lett.* **2012**, *100*, 161908.
[163] M. Shahinpoor, *Bioinspiration Biomimetics* **2011**, *6*, 046004.
[164] M. Shahinpoor, K. J. Kim, *Smart Mater. Struct.* **2001**, *10*, 819.
[165] E. Sinibaldi, G. L. Puleo, F. Mattioli, V. Mattoli, F. Di Michele, L. Beccai, F. Tramacere, S. Mancuso, B. Mazzolai, *Bioinspiration Biomimetics* **2013**, *8*, 025002.
[166] E. C. Freeman, *Ph.D. Thesis*, University of Pittsburgh, **2012**.
[167] E. Freeman, L. M. Weiland, in *Proc. of the ASME 2008 Conf. on Smart Materials, Adaptive Structures and Intelligent Systems*, Vol. *2*, (Ed: D. Brei) ASMEDC, Ellicott City, MD **2008**, pp. 559–567.
[168] T. Bhuyan, A. K. Singh, D. Dutta, A. Unal, S. S. Ghosh, D. Bandyopadhyay, *ACS Biomater. Sci. Eng.* **2017**, *3*, 1627.
[169] Y. Han, Y. Liu, W. Wang, J. Leng, P. Jin, *Soft Matter* **2016**, *12*, 2708.
[170] J. Li, Y. An, R. Huang, H. Jiang, T. Xie, *ACS Appl. Mater. Interfaces* **2012**, *4*, 598.
[171] T. Xiang, J. Hou, H. Xie, X. Liu, T. Gong, S. Zhou, *Nano Today* **2020**, *35*, 100980.
[172] M. Otake, Y. Kagami, M. Inaba, H. Inoue, *Rob. Auton. Syst.* **2002**, *40*, 185.
[173] A. Phadke, C. Zhang, B. Arman, C.-C. Hsu, R. A. Mashelkar, A. K. Lele, M. J. Tauber, G. Arya, S. Varghese, *Proc. Natl. Acad. Sci. USA* **2012**, *109*, 4383.
[174] M. Zhang, D. Xu, X. Yan, J. Chen, S. Dong, B. Zheng, F. Huang, *Angew. Chem., Int. Ed.* **2012**, *51*, 7011.
[175] J. K. Oh, R. Drumright, D. J. Siegwart, K. Matyjaszewski, *Prog. Polym. Sci.* **2008**, *33*, 448.
[176] K. G. Lee, J. Hong, K. W. Wang, N. S. Heo, D. H. Kim, S. Y. Lee, S. J. Lee, T. J. Park, *ACS Nano* **2012**, *6*, 6998.
[177] G. H. Kwon, Y. Y. Choi, J. Y. Park, D. H. Woo, K. B. Lee, J. H. Kim, S.-H. Lee, *Lab Chip* **2010**, *10*, 1604.
[178] M. C. Cushing, K. S. Anseth, *Science* **2007**, *316*, 1133.
[179] S. Iravani, R. S. Varma, *Green Chem.* **2019**, *21*, 4839.
[180] S. Schauer, M. Worgull, H. Hölscher, *Soft Matter* **2017**, *13*, 4328.
[181] G. Hao, Z. P. Xu, L. Li, *RSC Adv.* **2018**, *8*, 22182.
[182] E.-H. Liu, L.-W. Qi, Q. Wu, Y.-B. Peng, P. Li, *Mini-Rev. Med. Chem.* **2009**, *9*, 1547.
[183] Y. Pommier, C. Marchand, *Nat. Rev. Drug Discovery* **2012**, *11*, 250.
[184] X. Li, D. Zhang, V. J. Lynch-Holm, T. W. Okita, V. R. Franceschi, *Plant Physiol.* **2003**, *133*, 549.
[185] S. V. Pennisi, D. B. McConnell, L. B. Gower, M. E. Kane, T. Lucansky, *New Phytol.* **2001**, *150*, 111.
[186] X. Ma, L. Li, L. Yang, C. Su, Y. Guo, K. Jiang, *Mater. Lett.* **2011**, *65*, 3176.
[187] W. Wei, G.-H. Ma, G. Hu, D. Yu, T. Mcleish, Z.-G. Su, Z.-Y. Shen, *J. Am. Chem. Soc.* **2008**, *130*, 15808.
[188] A. S. Foster, *Protoplasma* **1956**, *46*, 184.
[189] H. Li, Y. Zheng, L. Qin, *Prog. Nat. Sci.: Mater. Int.* **2014**, *24*, 414.
[190] Z. Chen, R. Cao, S. Ye, Y. Ge, Y. Tu, X. Yang, *Sens. Actuators, B* **2018**, *255*, 2971.
[191] S. Reddy, E. Arzt, A. del Campo, *Adv. Mater.* **2007**, *19*, 3833.
[192] H. Xu, C. Yu, S. Wang, V. Malyarchuk, T. Xie, J. A. Rogers, *Adv. Funct. Mater.* **2013**, *23*, 3299.
[193] M. Ebara, K. Uto, N. Idota, J. M. Hoffman, T. Aoyagi, *Adv. Mater.* **2012**, *24*, 273.
[194] C.-M. Chen, S. Yang, *Adv. Mater.* **2014**, *26*, 1283.
[195] J. K. Park, S. Kim, *Lab Chip* **2017**, *17*, 1793.
[196] T. Lv, Z. Cheng, D. Zhang, E. Zhang, Q. Zhao, Y. Liu, L. Jiang, *ACS Nano* **2016**, *10*, 9379.
[197] Z. Cheng, D. Zhang, T. Lv, H. Lai, E. Zhang, H. Kang, Y. Wang, P. Liu, Y. Liu, Y. Du, S. Dou, L. Jiang, *Adv. Funct. Mater.* **2018**, *28*, 1705002.
[198] J. Wu, S. Balasubramanian, D. Kagan, K. M. Manesh, S. Campuzano, J. Wang, *Nat. Commun.* **2010**, *1*, 36.
[199] X. Xu, H. Li, D. Hasan, R. S. Ruoff, A. X. Wang, D. L. Fan, *Adv. Funct. Mater.* **2013**, *23*, 4332.
[200] M. Khatami, H. Alijani, M. Nejad, R. Varma, *Appl. Sci.* **2018**, *8*, 411.
[201] V. Mohammadzadeh, M. Barani, M. S. Amiri, M. E. Taghavizadeh Yazdi, M. Hassanisaadi, A. Rahdar, R. S. Varma, *Sustainable Chem. Pharm.* **2022**, *25*, 100606.

Rachmi Luthfikasari is a master student of Biosystems Engineering at Kangwon National University, South Korea. She received her bachelor's degree in Biology from University of Indonesia, Indonesia. Her research interest is biomimetic material and its application in tissue engineering.

Tejal V. Patil is a doctoral student of Biosystems Engineering at Kangwon National University, South Korea. She received her master's degree from Institute of Chemical Technology, Mumbai, India. Her research interest is development of biomaterials and tissue engineering.

Dinesh K. Patel is a postdoctoral research fellow at Institute of Forest Sciences, Kangwon National University, South Korea. He received his doctoral degree in Material Science and Engineering from Indian Institute of Technology, Banaras, India. His research interest is synthesis of biomimetic nanomaterials and their application in tissue engineering.

Sayan Deb Dutta is a doctoral student of Biosystems Engineering at Kangwon National University, South Korea. He reviewed his master's degree from University of Kalyani, India. His research interest is the synthesis of multifunctional nanomaterials for 3D printing and nanotheranostic applications for tissue engineering.

Keya Ganguly is a doctoral student of Biosystems Engineering at Kangwon National University, South Korea. She received her master's degree from Presidency University, India. Her research interest is development of nanoengineered scaffolding platform for smart biosensing and tissue engineering.

Maria Mercedes Espinal is a master student of Biosystems Engineering at Kangwon National University, South Korea.

Ki-Taek Lim is a professor of Biosystems Engineering, Kangwon National University, South Korea. He received his doctoral degree from Seoul National University, South Korea and joined as a postdoctoral research fellow at University of Arkansas, USA. His research interest is development of stimuli-responsive and smart cell culture system for nanomedicine and tissue engineering.